FROM THE DEPARTMENT OF CLINICAL SCIENCE, INTERVENTION AND TECHNOLOGY
Karolinska Institutet, Stockholm, Sweden

PANCREATIC DUCTAL ADENOCARCINOMA: COMPUTED TOMOGRAPHY FOR DIAGNOSIS, LOCAL STAGING AND PREDICTION OF POSTOPERATIVE COMPLICATIONS

Louiza Loizou

Karolinska Institutet

Stockholm 2015

All previously published papers were reproduced with permission from the publisher.
Cover image by Stefania Marconi.
Art images preceding paper 2 and 3 by Bertil Leidner and Anders Svensson.
Published by Karolinska Institutet.
Printed by E-Print AB 2015

ISBN 978-91-7549-868-3

To my parents, Simos and Yianna,
for all the sacrifices they made and make,
to fulfill my dreams.

ABSTRACT

Pancreatic ductal adenocarcinoma (PDAC) is a disease with a dismal prognosis, being the 4th leading cause of cancer deaths in Sweden and worldwide. The only potentially curative therapy is surgery. Unfortunately, by the time of diagnosis only 20% of patients have a resectable tumor and the overall 5-year survival rate does not exceed 5%. One of the main reasons for this is that some tumors are not detected, either because of small size or difficulty in delineation. Another reason is the underestimation or in some cases overestimation of the local tumor staging. These patients undergo an extensive but unnecessary operation or are withheld from potentially curative surgery, respectively. In some cases the patients develop serious postoperative complications, which can be predicted and perhaps avoided with proper preoperative planning. Technological advances in multidetector computed tomography (MDCT), combined with its wide availability, have made MDCT the modality of choice for PDAC imaging.

The overall purpose of this thesis was to investigate the role of MDCT in patients with PDAC in terms of (i) tumor diagnosis, (ii) local staging assessment and (iii) prediction of postoperative complications.

In **Study I,** we compared low-tube-voltage (80 kV) with normal-tube-voltage (120 kV) protocols regarding tumor detection by using a phantom that simulated the normal pancreatic parenchyma and hypovascular tumors. Our results showed that low tube-voltage significantly improves tumor detection.
In **Study II**, we evaluated 30 MDCT examinations of the pancreas in patients with PDAC in the pancreatic head, obtained according to our institution's standard protocol (120 kV and 0.75 g iodine (I)/kg body-weight). Based on our hospital's classification system, we investigated the interobserver agreement among radiologists in local tumor staging assessment and the correlation of this assessment to the surgical outcome. Our results showed almost perfect agreement among radiologists as well as an increased risk for vascular involvement with more advanced preoperative staging.
In **Study III**, we compared low-tube-voltage normal-iodine-load (80 kV and 0.75gI) with low-tube-voltage high-iodine-load (80 kV and 1gI) and with normal-tube-voltage normal-iodine-load (120 kV and 0.75gI) protocols in 30 patients with PDAC, regarding tumor conspicuity and local vessel involvement. Our results showed that low tube-voltage and high iodine-load significantly improve tumor conspicuity.
In **Study IV**, we correlated the pancreatic remnant volume (PRV) and pancreatic duct width (PDW) in 182 patients undergoing pancreaticoduodenectomy (PDE), to the risk for pancreatic leakage and fistula (PF) formation. Our results showed a significantly higher risk for PF in patients with high PRV and/or small PDW.

In conclusion, a high-quality preoperative MDCT is a very useful tool in the evaluation of PDAC in terms of tumor diagnosis, staging and prediction of postoperative complications. The low-tube-voltage high-iodine-load technique has the potential to improve tumor diagnosis and local staging.

LIST OF PUBLICATIONS

I. Holm J, Loizou L, Albiin N, Kartalis N, Leidner B, Sundin A. Low tube voltage CT for improved detection of pancreatic cancer: detection threshold for small simulated lesions. BMC Med Imaging. 2012 Jul 24; 12:20

II. Loizou L, Albiin N, Ansorge C, Andersson M, Segersvärd R, Leidner B, Sundin A, Lundell L, Kartalis N. Computed tomography staging of pancreatic cancer: a validation study addressing interobserver agreement. Pancreatology. 2013 Nov-Dec; 13(6): 570-5

III. L. Loizou, N. Albiin, B. Leidner, E. Axelsson, M.A. Fischer, A. Grigoriadis, M. Del Chiaro, R. Segersvärd, C. Verbeke, A. Sundin, N. Kartalis. Multidetector CT of pancreatic ductal adenocarcinoma: effect of tube-voltage and iodine-load on tumor conspicuity, vessel involvement and image quality. (Submitted to European Radiology - EURA-D-15-00660)

IV. Frozanpor F, Loizou L, Ansorge C, Segersvärd R, Lundell L, Albiin N. Preoperative pancreas CT/MRI characteristics predict fistula rate after pancreaticoduodenectomy. World J Surg. 2012 Aug; 36 (8): 1858-65

TABLE OF CONTENTS

LIST OF ABBREVIATIONS

CA	Celiac axis
CM	Contrast medium
CTDIvol	Computed tomography dose index volume
DE	Dual energy
DLP	Dose length product
DP	Distal pancreatectomy
ED	Effective dose
EUS	Endoscopic ultrasound
FNA	Fine needle aspiration
FOM	Figure of merit
FROC	Free-response receiver operating characteristics
GDA	Gastroduodenal artery
HA	Hepatic artery
I	Iodine
ISGPF	International Study Group for Pancreatic Fistula
ISGPS	International Study Group for Pancreatic Surgery
LL	Lesion localization
LLF	Lesion localization fraction
MDCT	Multidetector computed tomography
MRI	Magnetic resonance imaging
NCP	Non-contrast phase
NL	Non-lesion localization
NLF	Non-lesion localization fraction
NPV	Negative predictive value
PA	Protocol A
PB	Protocol B
PC	Protocol C
PD	Protocol D
PDAC	Pancreatic ductal adenocarcinoma
PDE	Pancreaticoduodenectomy

PDW	Pancreatic ductal width
PE	Protocol E
PET/CT	Positron emission tomography/computed tomography
PF	Pancreatic fistula
PPP	Pancreatic parenchymal phase
PPV	Positive predictive value
PRV	Pancreatic remnant volume
PS	Standard protocol
PV	Portal vein
PVP	Portal venous phase
ROC	Receiver operating characteristics
SA	Splenic artery
SMA	Superior mesenteric artery
SMV	Superior mesenteric vein
SV	Splenic vein
US	Abdominal ultrasound

1 INTRODUCTION

1.1 PANCREAS

The pancreas is a retroperitoneal organ representing the body's largest digestive gland with both endocrine and exocrine functions [1]. It has a firm, smooth, lobulated surface and is anatomically divided into the head, neck, body, tail and uncinate process. The neck, which is the portion between the head and the body, is situated anterior to the confluence of the portal vein (PV) and superior mesenteric vein (SMV) and is the anatomical landmark during the two most common pancreatic surgeries (pancreaticoduodenectomy-PDE or so-called Whipple operation and distal pancreatectomy-DP) [2]. The body and tail run transversely and slightly upwards with no clear-cut margin between them. The tail, which is the most lateral part of the gland, lies between the layers of the splenorenal ligament [2].

Embryologically, the pancreas arises from two buds of the endoderm at the level of the duodenal loop [3]. The small ventral bud, which gives rise to the inferior part of the head and the uncinate process, rotates dorsally and fuses with the dorsal bud, from which comes the superior part of the head, the body and the tail of the gland [3].

The size of the gland varies among populations of the same age and women tend to have smaller volumes than men [4]. During childhood and adolescence the pancreatic volume increases linearly with age, between 20-60 years reaches a plateau, and then declines thereafter [5]. Interestingly, while the total volume of the pancreas decreases, an increase in the anteroposterior diameter of the head is often observed [4].

The major part of the gland is exocrine, secreting enzymes for the digestion of carbohydrates, lipids and proteins [2]. The endocrine function is responsible for the glucose homeostasis, motility and function of the upper gastrointestinal tract [2].

The arterial blood supply of the pancreas derives from branches of the celiac axis (CA), superior mesenteric artery (SMA) and splenic artery (SA). The head of the pancreas and the uncinate process are supplied by the superior and inferior pancreaticoduodenal arcade [6]. The superior pancreaticoduodenal artery arises from the gastroduodenal artery (GDA), which is a branch of the common hepatic artery (HA), whereas the inferior pancreaticoduodenal artery arises from the SMA [7]. The SA follows a course along the superior margin of the body and tail and gives rise to the dorsal pancreatic artery, the pancreatic magna and the distal branches to the tail [7].

The venous drainage of the pancreas follows the arteries. Four major pancreaticoduodenal veins (anterior and posterior, superior or inferior pancreaticoduodenal veins) drain the head into the gastrocolic branch of the SMV, the PV, or the jejunal branch of the SMV [8]. Numerous veins drain the body and tail directly into the splenic vein (SV) [9].

Lymphatic drainage is extensive. Lymph capillaries originate around the pancreatic acini. The lymph vessels, likewise the veins, follow the arteries. Vessels from the tail and body drain mostly into the pancreaticosplenic lymph nodes [10]. Lymphatics from the neck and head drain into lymph nodes along the pancreaticoduodenal arteries, SMA and HA [10]. Occasionally there is direct drainage to the preaortic and CA lymph nodes [2].

1.2 PANCREATIC DUCTAL ADENOCARCINOMA

Pancreatic ductal adenocarcinoma (PDAC), although rare, is the 4th leading cause of cancer-related deaths worldwide [11; 12]. It represents 85-90% of all pancreatic neoplasms [13]. The only curative therapy is surgery with or without neo- or adjuvant radio/chemotherapy, but unfortunately, at the time of diagnosis only 20% of patients have a resectable tumor [14]. The overall 5-year survival rate is approximately 5% and it can reach 20% only after curative surgery [14]. These percentages have not altered significantly over the last two decades despite the technological developments in diagnostic imaging or the introduction of more aggressive surgical techniques [15]. It is estimated that during 2015 pancreatic cancer-related deaths will be almost as high as the reported new cases of pancreatic cancer (40,650 and 48,960, respectively) in the United States [15].

The main reasons for PDAC's dismal prognosis may include: (i) many patients seek health care too late, when the tumor is beyond cure, because the debut symptoms are often non-specific; (ii) some tumors are not detected, either because of small size or difficulty in delineation from the normal pancreatic parenchyma [16; 17]; (iii) the stage of the tumor is underestimated, which results in an extensive but unnecessary operation with high risk for postoperative complications and in the delayed application of other oncologic therapy [18], and (iv) sometimes the extent of the tumor is overestimated, which results in potentially curative surgery being withheld from these patients [19].

As already mentioned, the disease debuts with non-specific symptoms, such as abdominal epigastric pain radiating into the back, weight loss or new onset diabetes. Painless obstructive jaundice with pale stool, dark urine and pruritus are symptoms that usually make the patient seek health care but are relatively late symptoms depending on the location of the tumor [20]. Smoking and hereditary pancreatitis are two of the most common independent predictors of the disease [21].

1.3 PANCREATIC DUCTAL ADENOCARCINOMA IMAGING

Pancreatic imaging in patients with PDAC is mainly used for tumor diagnosis and staging. It is also used in selected cases for the detection and monitoring of postoperative complications as well as for detection of tumor recurrence. In this section, the role of the various imaging modalities of PDAC imaging will be discussed with the exception of multidetector computed tomography (MDCT), which is described separately in the next chapter.

1.3.1 Abdominal Ultrasound

Abdominal ultrasound (US) is usually the first-line, non-invasive, cost-effective diagnostic tool for patients with abdominal pain or obstructive jaundice [22]. Reported sensitivity in the detection of pancreatic cancer varies between 50 - 90% and is highly dependent on the operator's experience and the patient's body habitus [23]. Regarding the assessment of tumor resectability, a recent study yielded a 75% accuracy when the examination was performed by experienced ultrasonographers [24]. In our clinical experience and that of others [25], US plays an important role in the initial evaluation of patients with cholecystitis-like symptoms but has no role in the diagnosis or staging of pancreatic cancer.

PDAC typically appears as a solid hypoechoic lesion with ill-defined margins. When the tumor is located in the head of the pancreas, a "double duct" sign with dilatation of the common bile duct and the main pancreatic duct is often observed [26]. After the administration of intravenous contrast medium (CM), PDACs enhance poorly in all phases compared to the normal pancreatic parenchyma and the peripancreatic vessels, making detection and the resectability assessment more accurate [27].

1.3.2 Endoscopic Ultrasound

The main and well-established role of endoscopic ultrasound (EUS), due to its invasive nature, is the guided fine needle aspiration (FNA) from pancreatic lesions for cytology [28].

The role of EUS in diagnosis and preoperative management is not clear. According to one meta-analysis, EUS remains the most accurate method for detecting small (< 3 cm) pancreatic tumors, ampullary neoplasms and small (< 4 mm) bile duct stones [29].
Regarding tumor local resectability, assessment with EUS has shown sensitivity and specificity comparable to MDCT [28]. However, there are major limitations such as the assessment of the distant extent of the tumor, i.e. liver metastasis and peritoneal carcinomatosis.

1.3.3 Magnetic Resonance Imaging

The role of magnetic resonance imaging (MRI) in the diagnosis and staging of PDAC has been debated in recent years. No significant differences were observed

between CT and MRI images in the depiction of pancreatic carcinoma (sensitivity 95% vs 96%, respectively, and specificity 96%, in both) [30; 31]. However, the superiority of MRI for small liver metastases detection is indisputable (sensitivity 85 - 87% vs 69%) [30; 32].

The normal pancreatic parenchyma demonstrates low signal intensity on T2-weighted images and high signal intensity on pre-contrast T1-weighted images reflecting the high protein content of the exocrine part of the gland [33]. PDAC is hypointense on fat-suppressed, T1-weighted images before and after gadolinium contrast injection and has variable signal intensity on T2-weighted images [34]. On diffusion-weighted images (DWI), PDAC has restricted diffusion but this is not tumor-specific [35].

1.3.4 Positron Emission Tomography/Computed Tomography

The value of positron emission tomography/computed tomography (PET/CT) in pancreatic cancer is still controversial and no consensus has been reached on whether and when it should be applied [36]. [18F]-fluorodeoxyglucose (FDG) PET/CT is not superior to MDCT for the detection of local lymph node metastases [37]. However, a recent study has shown the superiority of PET/CT in the detection of distant metastases that are occult with MDCT [38]. Furthermore, it has higher sensitivity regarding bone metastasis detection but this is a rare manifestation of the disease [39]. Pancreatic malignancies usually have high FDG uptake and appear as “hot spots” within the pancreas [23].

1.4 MULTIDETECTOR COMPUTED TOMOGRAPHY OF PANCREATIC DUCTAL ADENOCARCINOMA

The best modality for PDAC imaging depends largely on local expertise, preference and availability. Recent technical advances in MDCT, permitting high spatial and temporal resolution imaging, combined with very wide availability, have made MDCT the preferred modality for the radiological evaluation of patients with PDAC [40; 41]. Moreover, the International Study Group of Pancreatic Surgery (ISGPS) [42] suggests that the preoperative evaluation of tumor resectability should be based on MDCT images.

In our institution at the Karolinska University Hospital in Huddinge, which serves as a tertiary referral center for pancreatic diseases, a triple-phase MDCT is considered the modality of choice in patients with suspected pancreatic cancer whereas MRI has the role of the problem-solving modality.

1.4.1 MDCT for Diagnosis

1.4.1.1 The role of MDCT in PDAC diagnosis

The overall sensitivity of MDCT in tumor diagnosis is reported to be between 86 - 97%. While MDCT is highly sensitive in detecting large tumors (up to 100% for tumors greater than 2 cm), the sensitivity is lower (60 - 77%) for tumors smaller than 2 cm [16; 17; 43]. Additionally, the tumor size, which is considered as an independent prognostic factor [44], may be underestimated in up to 75% of cases, according to a recently published study [45]. Furthermore, apart from the tumor size, it has been reported that up to 14% of PDACs show similar attenuation with the surrounding parenchyma, despite the adequate CT technique, which makes tumor detection quite challenging [46; 47].

1.4.1.2 Image characteristics during diagnosis

A triple-phase protocol with a non-contrast phase (NCP), a late arterial phase or a so-called pancreatic parenchymal phase (PPP) and a portal venous phase (PVP) is recommended [17]. The PPP is the optimal phase for detecting and delineating PDACs because of the higher attenuation difference between the hypovascularized tumor and the avidly enhanced parenchyma [48; 49]. An illustrative example is shown in Figure 1. Due to the high fibrous tissue content, PDAC is visualized as an ill-defined infiltrative lesion and shows slight and sometimes delayed contrast enhancement. Upstream, either main pancreatic or common bile duct dilatation as well as parenchymal atrophy are common (up to 70% of cases) [50] and in some patients, it may represent the only finding [51].

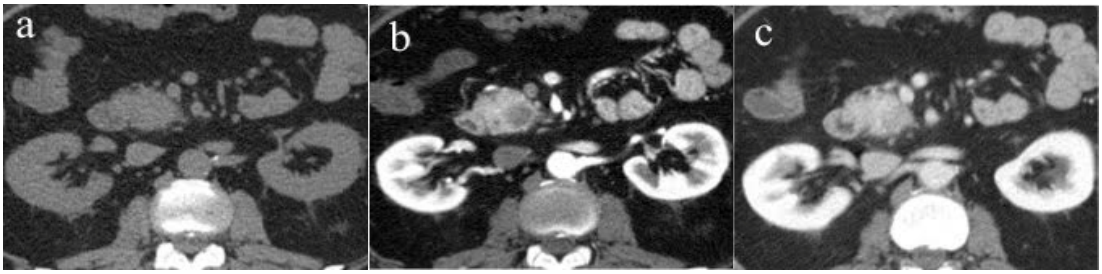

Figure 1: Axial MDCT images from a patient with ductal adenocarcinoma in the head of the pancreas in the non-contrast phase - NCP (a), the pancreatic parenchymal phase - PPP (b) and the portal venous phase - PVP (c). The hypovascularized tumor is not visible in the NCP. It may be suspected in the PVP but it is best delineated in the PPP.

1.4.2 MDCT for Local Staging

It is extremely important to use a common, internationally accepted classification system in order to provide both clinicians and researchers with a common language for pancreatic cancer staging. An optimal classification system should: (i) guide surgical planning, (ii) estimate prognosis, and (iii) evaluate treatment response.
Recent studies have shown that by using structured reports for the assessment of pancreatic MDCT, the omission of important information for the surgeons (i.e. vessel anatomy variants) is reduced, and this improves surgical planning [52; 53].

1.4.2.1 The role of MDCT in PDAC staging

Regarding the assessment of tumor surgical unresectability, several studies have demonstrated a high positive predictive value (PPV) with reported values reaching 100% (90 - 100%) [54; 55]. In practice, that means that almost no patient with resectable disease is withheld from potentially curative surgery. However, reported PPVs for the assessment of tumor local resectability have varied widely (52 - 96%) [54]. This means that there is a group of patients, with unresectable disease, who undergo an extensive operation with no benefit. A meta-analysis including 15 studies with an overall total of 1,015 patients has shown that the median probability of unresectable disease being incorrectly diagnosed as resectable is 40% [56]. Taking this data into consideration, 4 out of 10 patients undergo an unnecessary laparotomy. This meta-analysis includes older studies with incomplete CT protocols and older CT scans. More recent studies have yielded higher specificity of tumor resectability reaching 90% [57].

1.4.2.2 Image characteristics during staging

If distant metastases (i.e. liver or lung) or peritoneal carcinomatosis are absent, a detailed description of the major peripancreatic vessels' involvement is mandatory in order to assess the local tumor staging and thus tumor resectability. The two main parameters traditionally used for evaluating vessel involvement are the grade of the circumferential surface [58] and the length of the vessel with which the tumor is contiguous [59]. In order to avoid inconsistency in the description of vessel involvement in this thesis, the MD Anderson's Cancer Center definition has been

adopted: if tumoral involvement of the vessel circumference is ≤180° or >180°, the word abutment or encasement is used, respectively [59].

1.4.2.3 Different Classification Systems

The World Health Organization (WHO) [60] and the American Joint Committee on Cancer (AJCC) [61] recommend the "TNM" classification system for pancreatic cancer staging, where T refers to tumor, N to lymph nodes and M to metastases. According to this classification, the T status divides the tumors as intrapancreatic (T1: <2 cm and T2: >2 cm) and extrapancreatic (T3: without or T4: with SMA or CA involvement). Even though this classification system is a very useful tool for postoperative evaluation of the patient's prognosis, it does not include the role of venous involvement nor have any precise definition of "vessel involvement", which make it insufficient for preoperative assessment of tumor resectability [62].

Lu and Loyer were almost simultaneous pioneers correlating the tumor's relationship to the main peripancreatic vessels and tumor resectability. Lu et al. described the likelihood of tumoral vascular involvement based on the percentage of circumferential surface contact between the tumor and the vessel, concluding that more than 180° of tumor-vessel contact is highly specific for tumor unresectability [58]. Loyer et al. proposed a more descriptive classification, again based on the extension of the hypodense tumor and its relationship to the main peripancreatic vessels (Table 1) [63]. Both studies showed an increased risk for vessel involvement and therefore an increased risk for the need for vessel resection or tumor unresectability with increasing circumferential tumoral involvement of the vessel. However, these classifications do not take into account the length of the vessel that is contiguous to the tumor or the differences between venous and arterial involvement. Additionally, they do not differentiate between per continuitatem tumor growth around the vessel and perivascular stranding, which does not necessarily consist of tumoral tissue [64].

Table 1. Loyer's classification of vascular involvement in PDAC

Type	**Tumor's relationship to the major peripancreatic vessels**
A	Fat plane separates the tumor from adjacent vessels
B	Normal parenchyma separates the tumor from adjacent vessels
C	Tumor against the adjacent vessel forming a convexity
D	Tumor against the adjacent vessel forming a concavity
E	Tumor encircling the adjacent vessel
F	Tumor occluding the adjacent vessel

Loyer et al. Abdominal Imaging. 1996 May-June; 21(3): 202-6

The definition of pancreatic cancer resectability has changed over recent decades. This is mainly due to two reasons: firstly, due to the development of new surgical and more aggressive therapeutic approaches allowing vessel resection and reconstruction with survival rates comparable with those of patients undergoing surgery without vessel resection [65] and secondly, due to the introduction and wide use of neoadjuvant therapies with high probability for negative resection margins (R0) after operation. These reasons necessitated the introduction of new classification systems that have an impact on the immediate therapeutic management.

In 2006, the MD Anderson's Cancer Center introduced a new classification system by adding a third category of tumors other than "resectable" and "unresectable" ones, called "borderline" (Table 2) [59]. Their main goal was to optimize preoperative treatment and minimize the risk of falsely categorizing a tumor as unresectable/locally advanced. They stated that the end point for the analysis of tumor resectability should be the negative resection margins (R0). Regarding SMA, they stated that vessel abutment or periarterial stranding categorize the tumor as "borderline" because complete resection is more likely. Even short-segment encasement of the HA, usually at the GDA origin, allows vascular resection with a high probability of R0-resection.

Table 2. MD Anderson Cancer Center's criteria for resectability assessment of pancreatic cancer

Vessel	**Resectable**	**Borderline**	**Locally advanced**
SMA	No extension	Abutment Periarterial stranding or convexity against the vessel	Encased
CA/HA	No extension	Short-segment encasement/abutment of HA typically at the GDA origin	Encased and no technical options for reconstruction usually because of extension to the CA
SMV/PV	Patent	Short-segment occlusion with suitable vessel above and below	Occluded and no technical option for reconstruction

SMA: superior mesenteric artery; CA: celiac axis; HA: hepatic artery; SMV: superior mesenteric vein; PV: portal vein; GDA: gastroduodenal artery.

Varadhachary et al. Annals of surgical Oncology 2006 Aug; 13(8): 1035-1046

In 2009, MD Anderson Cancer Center's classification system was adopted by the National Comprehensive Cancer Network (NCCN) with minor changes (Table 3) [66]. The main difference between these two classification systems is that abutment or encasement of SMV/PV is considered as "borderline" by the latter and straightforward resectable by the former.

Table 3. The National Comprehensive Cancer Network's criteria for resectability assessment of pancreatic cancer (version 1.2014)

Resectable	**Borderline resectable**	**Unresectable**
No distant metastasis No radiographic evidence of SMV/PV distortion	No distant metastasis SMV/PV involvement with distortion, narrowing or occlusion with suitable vessel above and below allowing resection and replacement	Distant metastasis Unreconstructible SMV/PV occlusion
Clear fat planes around CA, HA and SMA	GDA encasement up to HA with either short-segment encasement or abutment of the HA SMA abutment	SMA encasement CA abutment/encasement Aortic or IVC encasement or invasion

CA: celiac axis; GDA: gastroduodenal artery; HA: hepatic artery; IVC: inferior vena cava; PV: portal vein; SMA: superior mesenteric artery; SMV: superior mesenteric vein.

Tempero et al. J Natl Compr Canc Netw 2014 Aug; 12(8): 1083-93

These resectability criteria are given only for PDAC in the head of the pancreas. However, the presence of CA abutment/encasement does not preclude tumor resection in tumors located in the body and tail of the pancreatic gland [67]. In those cases en-bloc tumor and CA resection is recommended if the SMA, GDA and proper HA are free from the tumor.

1.4.2.4 Our Hospital's Classification System

In recent years a CT-based classification system has been introduced at the Karolinska University Hospital, based on principles of surgical resectability (Table 4). It takes into consideration both venous and arterial involvement with regard to the vessel circumference and length that is contiguous to the tumor. The importance of both parameters (circumference, length) differs between arteries and veins: i.e. even up to 360° involvement of a short SMV/PV segment is easier to deal with compared with corresponding involvement of the SMA or CA. Furthermore each category is correlated to a therapeutic management process. Based on radiological imaging, tumors in category A1 do not attach to any major vessel and it is considered unlikely that any vessel resection would be needed. Tumors in category A2 abut a limited segment of SMV/PV and vein resection is potentially required. Tumors in categories B1 and B2 encase a short segment of SMV/PV or abut a short segment of HA, respectively. Vessel resection is more probable. Tumors in category C show a more advanced vessel involvement and neoadjuvant therapy is recommended in most of these cases. Finally, category D tumors are considered locally advanced/unresectable and palliative therapy is almost always offered.

Table 4. Our hospital's classification for resectability assessment of pancreatic cancer

	Vein-SMV/PV	Artery	Management
A1	None	None	Primary resectable without vessel reconstruction
A2	≤180°	None	Primary resectable with minor risk of vein reconstruction
B1	>180° and ≤2cm	None	Primary resectable with probable need of vascular reconstruction
B2	Any of the above	HA≤180° and ≤2cm	
C	>180° and >2cm &/or	SMA or CA ≤180° and ≤2cm	"Borderline": probably resectable after neoadjuvant therapy
D	Total occlusion or encasement of mesenteric branch	HA or SMA or CA >180° or >2cm or encasement of mesenteric branching	Unresectable

SMV: superior mesenteric vein; PV: portal vein; HA: hepatic artery; SMA: superior mesenteric artery; CA: celiac axis.

1.4.3 MDCT for Prediction of Postoperative Complications

PDE remains the only curative therapy for patients with PDAC but it is associated with significant postoperative morbidity [68]. The most common complication responsible for this increased morbidity is the formation of a postoperative pancreatic fistula (PF) due to leakage from the pancreatico-enteric anastomosis [69]. The PF is graded from A to C based on the definition of the International Study Group on Pancreatic Fistula (ISGPF) [70]. According to this classification, grade A is the presence of a biochemical leakage. Biochemical leakage is defined as the output containing pancreatic amylase on or after the third postoperative day from a surgically positioned drain, displaying pancreatic amylase more than three times the upper serum reference value. Grade B is defined as clinically significant leakage such that therapeutic intervention is required. In Grade C severe clinical sequelae are present.

Several risk factors have been defined and validated, such as soft or fatty pancreas and small caliber pancreatic duct [71]. Most of these factors can only be objectively assessed at the time of surgery and are, by necessity, observer-dependent to a certain degree. The role of somatostatin analogs as inhibitors in the secretion of pancreatic digestive juices has not been established.

Modern radiological techniques may facilitate the risk prediction of PF formation in a preoperative setting [72]. A recent study at our institution suggested an increased PF risk after DP in patients presenting with large pancreatic remnant volume (PRV) and small radiological pancreatic duct width (PDW) [73].

1.4.4 MDCT Protocol Issues

As mentioned above, the best phase for PDAC diagnosis and delineation is the PPP where the attenuation difference between the normal pancreatic parenchyma and the tumor is highest. The role of PVP is limited to the assessment of the tumor's relationship to the main peripancreatic veins (PV/SMV) and to the evaluation of the hepatic parenchyma for detecting liver metastases. Two parameters influencing the pancreas-to-tumor attenuation difference are the tube voltage of the scanner and the total iodine load of the injected CM.

1.4.4.1 Parameters regarding the CT scanner: tube voltage

Tube voltage at 120 kV is considered standard in abdominal imaging at our institution and many others [74-77]. By reducing tube voltage from 120 kV to 80 kV, the mean photon energy of the X-ray beam is reduced from 56.8 to 43.7 keV, which is closer to the k-edge of iodine (33.2 keV). This phenomenon leads to higher X-ray absorption and, consequently, to higher attenuation of materials with a high atomic number such as iodine-containing structures [78]. This attenuation increase is achieved by an increased photoelectric effect (complete X-ray absorption) and decreased Compton scattering (X-ray scatter with fractional loss of X-ray energy) [79]. In addition, low-tube-voltage CT scanning has the ability to decrease the radiation dose, which is of major clinical importance. This principle has been used in thoracic [80] and heart [81] CT as well as in CT examinations of patients with low body mass index and of children [82]. In recent years, the technique has also been used to improve CT angiography of the pulmonary arteries [83] and the detection of hypervascular liver lesions [78]. Recently, a dual-energy (DE) MDCT study showed potential improvement in tumor conspicuity at 80 kV in terms of optimized pancreatic and peripancreatic vasculature enhancement [84]. However, the main drawback of low-tube-voltage MDCT is the increased image noise, which may have an impact in image quality.

1.4.4.2 Parameters regarding the contrast medium

The main parameters regarding CM are the total iodine load, the iodine concentration, the injection rate and duration as well as the scan delay.

The patient's body weight is correlated to the pancreatic and liver parenchymal enhancement: in heavier patients the enhancement is significantly lower compared to thinner patients if the same fixed volume of CM is administered [85]. For this reason a body-weight-tailored CM dosage is preferable rather than a fixed dosage [86; 87] due to comparable enhancement between thinner and heavier individuals.

The volume of the injected CM is subject to considerable variation and has traditionally been determined empirically. Heiken JP et al. showed that the volume should be at least 0.52g Iodine (I)/kg body weight for optimal liver attenuation and detection of hypovascular liver metastasis [88]. Yamashita et al. have shown that 0.75g I/kg body weight is superior to 0.6g I/kg and 0.45g I/kg body weight for liver and pancreatic imaging, respectively [89].

An increase in the iodine concentration –with the total iodine mass and injection rate kept constant– leads to shorter injection duration, smaller CM volume and higher iodine mass per unit time. Consequently that means earlier and greater peak aortic enhancement, in the time-density curve, without any significant effect on the parenchymal enhancement of the liver [90]. For instance, if we administer a highly concentrated CM – 400mg/ml – to a patient weighting 70 kg at a body-weight-tailored dosage of 0.75gI/kg and a fixed injection rate of 5ml/s, the total CM volume should be 130 ml and the injection duration 26s. If we choose the same CM at a lower concentration – 300mg/ml – the volume should be increased at 175 ml and, consequently, the injection duration should be prolonged at 35s.

The enhancement kinetics of the pancreas follows the arterial dynamics due to its entirely arterial blood supply from branches direct from the abdominal aorta [91]. Several studies have revealed the superiority of high concentration CM in terms of pancreatic parenchymal and peripancreatic vessel attenuation [92-94]. In addition, another advantage of a highly concentrated CM is the shorter injection time for a given volume [92].

Apart from CM concentration, the second most important parameter influencing the arterial enhancement is the CM injection rate. Schueller et al. have shown that a high injection rate (8ml/s) compared to a low one (4ml/s) of a fixed CM volume at an individualized scan delay (using bolus tracking), leads to a more rapid iodine load and to an increase in the magnitude of the peak pancreatic parenchymal attenuation. However, the pancreatic tumor attenuation does not differ significantly, which contributes to an increase in the parenchyma-to-tumor contrast [95]. Conversely, the magnitude of liver enhancement reaches a “plateau” with relative low injection rates (>2 ml/s), which means that liver parenchymal attenuation is independent of the injection rate and, thus, cannot be optimized accordingly [91]. Moreover, a high injection rate provides greater temporal separation between the PPP and PVP and this distinct phase separation is beneficial for multiphase scanning of the liver and pancreas [90].

At this point it is important to emphasize that changing the iodine concentration of the CM has the same proportional effect on arterial enhancement as changing the injection rate [90; 91].

The injection duration is defined as the CM volume divided by the injection rate. If the volume of the injected CM is relative high (i.e. if we administer body-weight-tailored

dose in heavier patients) and the injection rate is fixed, the injection duration will be prolonged with the risk that the scanning will start during the CM injection. For that reason fixed injection duration is preferable than fixed injection rate [96] especially in the cases of body-weight-tailored dosages. Yanaga suggested that using fixed injection duration in body-weight-tailored dosage protocols reduces the variation in the aortic peak time and aortic peak enhancement value [85]. The arterial and thus pancreatic enhancement increases cumulatively with the injection duration [91].

Scan timing is critical. A recent study revealed that 20-second and 30-second delays (with a body-weight-tailored volume and injection rate of 4ml/s) after the aortic transit time (150 HU) are superior to 10 seconds, whereas the pancreatic enhancement and the tumor-to-parenchyma contrast are higher [97].

In summary, a high injection rate of a highly concentrated CM at a fixed duration leads to an increase in the magnitude of peak vascular enhancement and to a better separation of the arterial and venous phases. However, the volume of the injected CM contributes foremost to the magnitude of liver enhancement. Taking into consideration the literature mentioned above, the optimal combination of CM parameters could be a body-weight-tailored dosage of 0.6 - 0.75g/I of a highly concentrated CM (more than 300mg/ml) that is injected at a high injection rate with at least a 20-second delay after the aortic transit time.

2 AIMS

The aims of this thesis were to investigate the role of MDCT in the:

1. **Detection** of PDAC by comparing normal- with low-tube-voltage imaging protocols **(Studies I and III)**

2. Assessment of **local tumor staging** by

a. Estimating the interobserver agreement among radiologists in assessing vessel involvement and predicting resectability using a normal-tube-voltage protocol and our institution´s classification system **(Study II)**
b. Comparing normal- with low-tube-voltage protocols in assessing vessel involvement **(Study III)**, and

3. **Prediction** of postoperative complications by correlating PRV and PDW with the risk of pancreatic leakage and fistula formation after PDE **(Study IV)**.

3 METHODS AND MATERIALS

Studies II, III and IV were approved by the regional ethics review board. An ethics permit was not needed for Study I.

3.1 STUDY POPULATION

Study I

One hundred simulated patient cases were created by using a phantom, which simulated the normal pancreatic parenchyma (Catphan® 600, The Phantom Laboratory, Salem, USA). The phantom was mounted into a body annulus (CTP579) to better simulate the size of the human trunk. In 57 of these cases, 1 to 3 spherical hypodense lesions were digitally inserted in random positions: 2, 3, 4, 5, 6, 8 and 10 mm in diameter.

Study II

Thirty patients (18 men and 12 women, mean age 68 years) were recruited retrospectively, between October 2006 and December 2010, from a register of 277 consecutive patients undergoing PDE for various pathologies. Inclusion criteria: (i) CT examination of the pancreas according to our institution's standard protocol (PS) (Table 6), (ii) patients assessed as having a potentially resectable hypovascularized tumor in the pancreatic head by the multidisciplinary tumor board and (iii) histopathologically verified PDAC. Exclusion criterion: administration of neoadjuvant therapy.

Study III

Thirty patients (14 men and 16 women, mean age 66 years) were recruited prospectively, between February 2010 and September 2014, from 235 consecutive patients assessed as having a potentially resectable hypovascularized pancreatic tumor by the multidisciplinary tumor board. Informed consent was obtained from each patient. Inclusion criterion: histopathologically verified PDAC. Exclusion criteria: (i) body weight higher than 85 kg, (ii) estimated GFR lower than 60 ml/min/1.73 m^2, (iii) undergoing neoadjuvant therapy. The tumor was located in the pancreatic head in 25 patients and in the body/tail in the remaining five patients. Data from a previous study on attenuation differences between parenchyma and tumor in patients with PDAC were used for performing power analysis [79].

Study IV

One hundred eighty two patients (94 men and 88 women, mean age 66 years) were recruited retrospectively, between September 2007 and November 2010, from a register (the same as in Study II) of 197 consecutive patients undergoing PDE for various pathologies. Inclusion criterion: presence of an adequate CT/MR examination of the pancreas. Exclusion criteria: (i) administration of neoadjuvant therapy and (ii) extended resection.

3.2 IMAGE ACQUISITION

Our institution's 64-channel MDCT scanners (LightSpeed VCT or LightSpeed VCT XTE, GE Healthcare, Milwaukee, USA) were used for all the CT examinations in Studies I, II and III. In Study IV, examinations from different institutions were included as long as the image quality for the study purpose was adequate.

Iomeprol 400 mg I/ml (Iomeron-400, Bracco Imaging SpA, Milan, Italy) or iodixanol 320 mg I/ml (Visipaque-320, GE Healthcare, Chalfont St. Giles, UK) were the two non-ionic iodinated CM used in Studies I, II and III. In Study IV the concentration of the CM was variable (320-400 mg I/ml).

Study I

The Catphan® 600 phantom was scanned 3 times with 3 different protocols: protocol A (PA), protocol B (PB) and protocol C (PC) as described in Table 5. In PA, the tube voltage was set at 120 kV. In PB and PC the tube voltage was decreased to 80 kV. In PB, the radiation dose was kept the same as in PA, while in PC, it was increased to achieve the equivalent image noise as in PA. All the other scanning parameters not mentioned in Table 5 were kept constant and were the same as in the PPP of our institution's PS (Table 6). The reconstruction slice thickness and interval were 3 mm and 1.5 mm respectively, corresponding to the PS's reconstructions with a narrower FOV. The total number of images per simulated patient case was 21.

The attenuation of the simulated normal pancreatic parenchyma at PA (120 kV) was set at 130 (SD=3.5) HU after measurements in PPP in 15 clinical pancreatic MDCT examinations according to PS (120 kV and 0.75 g I/kg body-weight). We assumed that the simulated lesions' attenuation differed from the background by only 20 HU and thus the lesions' attenuation was set at 110 HU. To estimate the corresponding attenuation for the parenchyma and the lesions at 80 kV, six different concentrations of CM (Iomeron-400) were diluted with water (1.1, 2.2, 3.2, 4.3, 5.4 and 6.5 mg I/ml water) in standard 10 ml plastic vials. These were inserted into the center position of a phantom (RMI Model 461A, Gammex/RMI, Middleton, USA), which was scanned at 120 kV and 80 kV. The attenuation values were plotted against the iodine concentration and correlated linearly (Figure 2). The corresponding attenuation values for the lesions and the parenchyma at 80 kV were 183 HU and 217 HU, respectively.

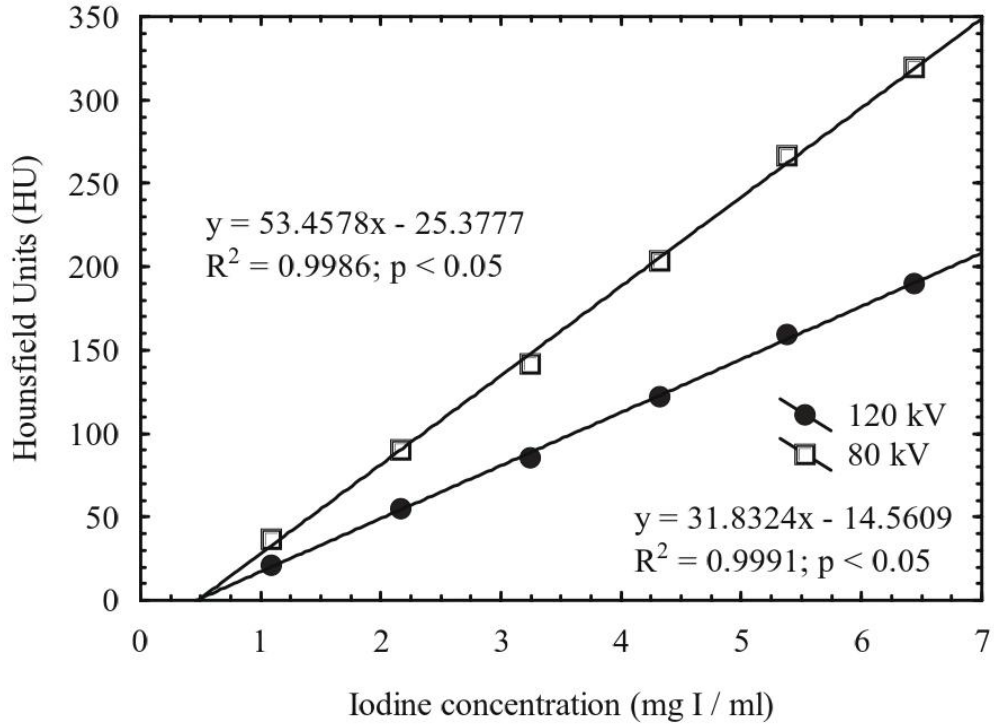

Figure 2. The mean attenuation (HU) for the six test tubes containing different iodine concentrations scanned at 120 kV and 80 kV.

Study II

All 30 patients underwent a CT examination of the pancreas according to our institution's PS (Table 6).

Study III

All 30 patients underwent two CT examinations of the pancreas. Following a CT examination according to the institution's PS (n=30), patients were randomized to two groups: (i) protocol D (PD, n=14; 80 kV and 0.75 g I/kg body weight) and (ii) protocol E (PE, n=16; 80 kV and 1 g I/kg body weight). The mean time interval between the two CT examinations was 15 (SD=7.5) days. The three protocols are briefly described in Table 6. For each patient, the serum creatinine level was measured before every examination and three days after the second examination. None of the patients showed signs of contrast-induced nephropathy.

Study IV

From the 182 patient examinations, 167 were MDCT and the remaining 15 MRI. All the examinations included at least a PPP and a PVP. The slice thickness varied between 3 mm (with a reconstruction interval of 1.5 mm) and 5 mm (with a reconstruction interval of 2.5 – 5 mm).

3.3 SCANNING PROTOCOLS

Our institution's PS as well as PA, PB, PC, PD and PE are illustrated in Tables 5 and 6.

Table 5. CT protocols in Study I

Protocol	Tube voltage (kV)	Tube current (mA)	CTDIvol (mGy)	Noise (HU)
PA	120	160	15	15
PB	80	500	15	17
PC	80	675	20	15

PA: protocol A; PB: protocol B; PC: protocol C; CTDIvol: computed tomography dose index volume.

Table 6. Our institution's standard protocol (PS) used in Studies II and III and Protocol D (PD) and Protocol E (PE) used in Study III

Protocol	Standard (PS)	PD	PE
Preparation	Fasting for 4 hours		
Oral Contrast	1,000 ml tap water, 30 min prior to examination		
Intravenous Contrast			
a. volume - **gI/kg body weight**	0.75	0.75	1
b. injection duration - **s**	25	25	25
c. I concentration - **mg/ml**	400/320	400/320	400/320
d. NaCl flush	50 ml-5ml/s	50 ml-5ml/s	50 ml-5ml/s
Scan timing and range			
a. NCP	Upper abdomen		
b. PPP	Upper abdomen: 20 s after bolus tracking reached 160 HU in the aorta at the level of the first lumbar vertebra		
c. PVP	Upper abdomen and pelvis: 25 s after the end of PPP scan		
Scanning parameters	PPP/PVP	PPP/PVP	PPP/PVP
a. collimation **(mm)**	0.625	0.625	0.625
b. table feed **(mm)**	20/39	20/39	20/39
c. tube voltage **(kV)**	120	80	80
d. tube current **(mA)**	ATCM	ATCM	ATCM
e. rotation time **(s)**	0.6	0.6	0.6
f. pitch	0.5/0.98	0.5/0.98	0.5/0.98
g. kernel	soft	soft	soft
Reconstructions	Axial, coronal and sagittal		
a. slice thickness	5 mm (& 3 mm with narrower FOV focused on pancreas)		
b. interval	2.5 mm (& 1.5 mm with narrower FOV focused on pancreas)		

I: Iodine; NCP: non-contrast phase; PPP: pancreatic parenchymal phase; PVP: portal venous phase; ATCM: automatic tube current modulation; FOV: field of view.

3.4 IMAGING ASSESSMENT

A standard picture archiving and communicating system (PACS) workstation (Sectra, Linköping, Sweden) was used for imaging assessment in all studies.
In addition, a Voxar® 3D workstation (Toshiba Medical Visualization Systems, Edinburgh, UK) with 3D segmentation and volume calculation was used for the PRV estimation in Study IV.

Study I
Three radiologists, with 24, 21 and 7 years of experience in the interpretation of CT examinations, blinded to the examination protocols and lesion characteristics, evaluated the 100 cases per protocol, independently and twice: first with fixed and then with free window settings. However, they were not allowed to use the zoom tool. To minimize the memory effect, for each protocol and each session the 100 cases were rearranged.

For each protocol and case each reader:
(i) marked the suspicious lesion/lesions with an arrow and
(ii) graded the confidence level on a four-point scale (1: probably not a lesion, 2: possibly a lesion, 3: probably a lesion, 4: definitely a lesion).

Study II
Nine radiologists, grouped as trainees, experienced and experts according to their years of experience in abdominal imaging (1-2 years, 5-6 years and >10 years, respectively) blinded to the surgical outcome, evaluated the 30 cases, independently. They were free to change the window settings and the zoom level at their preference as they would in clinical practice.

For each examination, they assessed the tumor involvement of the major peripancreatic vessels (PV/SMV, CA, HA and SMA) as well as of the mesenteric venous or arterial branching, addressing the:
(i) maximal percentage of the circumference, and
(ii) maximal length that was contiguous to the tumor.

Based on these evaluations, the tumors were classified by one of the readers into a category according to our hospital's classification system (Table 7).
For the correlation to the surgical outcome, consensus between three of the nine readers was obtained in those cases where less than 6 readers classified the tumor in the same category.
Finally, for the correlation to the R0 rate (%) and median survival the categories were grouped due to the small sample size: group 1, primarily resectable tumors with no contact to major peripancreatic vessels (category A1); group 2, primarily resectable tumors with limited contact to major peripancreatic vessels (categories A2, B1 and B2); and group 3, primarily non-resectable tumors (categories C and D).

Study III

Two radiologists with 15 and 6 years' experience in abdominal imaging, blinded to the examination protocols as well as to the surgical and histopathological findings, assessed all 60 examinations independently in random order for the qualitative analysis.

For each protocol and examination, each reader assessed:

(i) the tumor delineation on a four-point-scale (1: absent, 2: poor, 3: clear, 4: sharp),

(ii) the tumor involvement of the major peripancreatic vessels (PV/SMV, CA, HA and SMA) as well as of the mesenteric venous or arterial branching. The vessels were considered encased/abutted if more/equal or less than 180° of their circumference was in contact with the tumor, based on the criteria defined earlier [58] and as in Study II, and

(iii) the image quality on a four-point scale (1: poor, 2: acceptable, 3: good, 4: excellent).

The image quality was based on the sharpness of demarcation of the upper abdominal organs, the clarity of the mesenteric fat and the overall diagnostic impression.

A third radiologist with 3 years' experience in abdominal imaging assessed the images for the quantitative analysis.

For each protocol, examination and contrast-enhanced phase she measured the:

(iv) attenuation of the normal pancreatic parenchyma,

(v) attenuation of the tumor, and

(vi) standard deviation of the attenuation of the subcutaneous fat in the anterior abdominal wall.

The measurements were obtained by manually drawing three circular regions of interest (ROIs) to encompass as much of the parenchyma, tumor and subcutaneous fat as possible in the axial plane. Areas of necrosis, cystic formations, dilated ducts and vessels were avoided. For each patient, measurements were performed simultaneously and at the same level on both examinations and imaging phases to ensure consistency. The three measurements per parenchyma and tumor were averaged and used for the estimation of the:

(vii) parenchyma-to-tumor attenuation difference,

(viii) parenchyma-to-tumor contrast-to-noise ratio (CNR), using the formula:

CNR = (mean parenchyma - mean lesion attenuation)/noise, whereby noise was the mean value of the standard deviation (SD) of the subcutaneous fat attenuation, and

(ix) figure of merit (FOM) using the formula: $FOM = CNR^2/ED$ [84], whereby ED is the effective radiation dose. The FOM was estimated because direct comparison of the CNRs between the different protocols was not possible due to the fact that the radiation dose could not be kept constant when ATCM was applied.

Study IV

Two radiologists with 20 and 2 years' experience in abdominal imaging, blinded to the postoperative outcome, calculated in consensus:

(i) the PRV – the pancreatic volume at the left of the SMV – and

(ii) the PDW – at the transection line.

The volumetric analyses were performed in the axial plane (Figure 3) and in the contrast phase with the best delineation of the parenchyma (PPP in most of the cases) from the surrounding vessels. In 10 of the patients, the two radiologists calculated the volume separately and the interindividual variation was less than 10%.

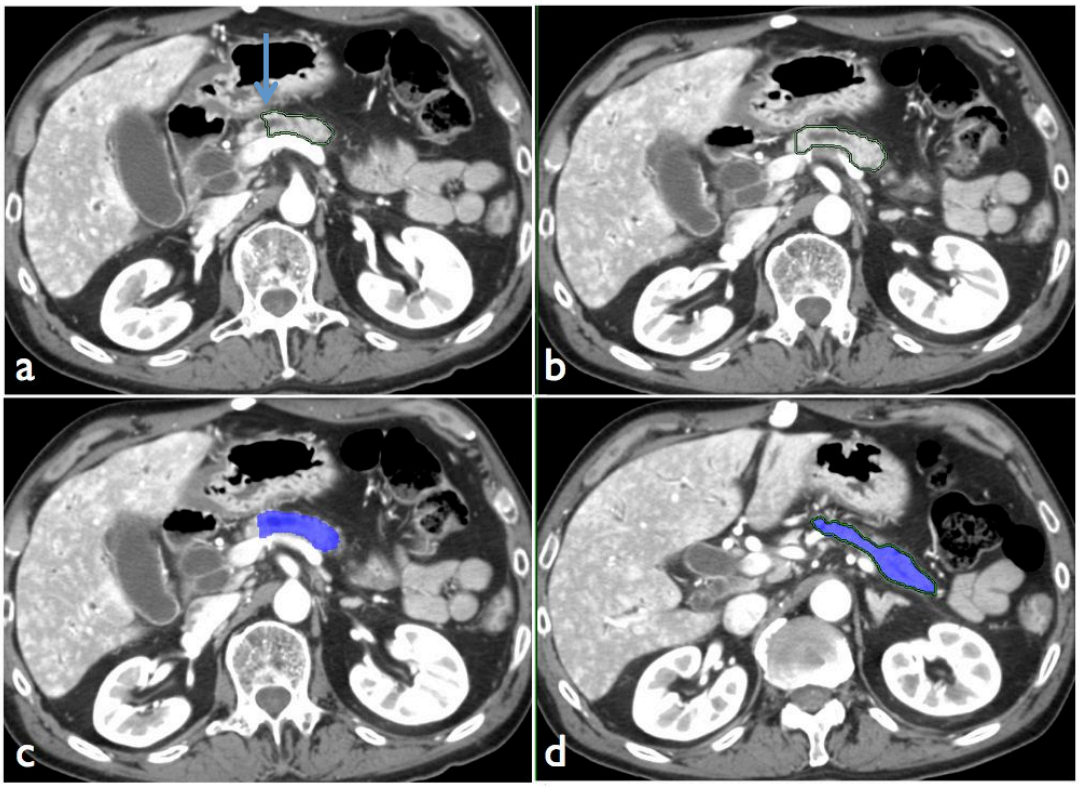

Figure 3: This is a CT examination performed according to our institution's standard protocol (PS) in a patient with ductal adenocarcinoma in the head of the pancreas. The four images show how the pancreatic remnant volume was estimated. With a semiautomatic segmentation technique, the pancreas can be delineated (green line), first at the level of the alleged resection line (blue arrow) and then several sections toward the tail (image b). The intermediate sections are automatically bordered (blue areas).

3.5 CLASSIFICATION SYSTEMS

In Study II, our hospital's classification system (Table 4) was applied for both the interobserver variability assessment and the correlation to the surgical outcome.
In Study III, the correlation of the major peripancreatic vessels' involvement with the surgical and histopathological outcome was based on the criteria proposed by Lu et al. [58] The vessels were considered encased/abutted if more/equal or less than 180° of their circumference was in contact with the tumor.

3.6 SURGICAL PROCEDURE

In all clinical studies (II, III and IV), all patients underwent surgical exploration with curative intent. Experienced and fully trained pancreatic surgeons familiar with the techniques of major vessel resection and reconstruction performed all the operations. The pre- and perioperative management was standardized as far as possible.
In Study II, 28 of the 30 patients underwent PDE (of these, 10 with SMV/PV resection, one with HA resection and one with HA and SMV/PV resection) and two patients underwent palliative by-pass surgery (due to vessel involvement).
In Study III, 23 out of the 30 patients underwent PDE (of these, eight with SMV/PV resection and one with SMV/PV and HA resection), two DP (of which one underwent SMV/PV resection and en-bloc CA resection) and five patients had palliative by-pass surgery (due to occult liver metastases and/or peritoneal carcinomatosis).
In Study IV, all 182 patients underwent PDE.
The mean time between examination and surgery was 23 (SD=14) days, 19 (SD=9) days and 40 (SD=29) days for Studies II, III, and IV, respectively.

3.7 HISTOPATHOLOGICAL ANALYSIS

All the specimens were evaluated in a standardized manner [98].
In Studies II and III, all the patients included had a histopathologically verified PDAC.
In Study III, the resected vessel segments were evaluated for the presence of microscopic wall infiltration. Of the 10 patients undergoing SMV/PV resection, eight showed evidence of wall infiltration whereas in both patients undergoing HA and CA perivascular tumor infiltration was found.
In Study IV, the majority of the patients (133/182, 73%) were diagnosed with PDAC. The next three most common diagnoses were neuroendocrine tumor (10/182, 5.5 %), pancreatitis (12/182, 6.6 %) and IPMN (10/182, 5.5 %). The rest of the diagnoses were gastric cancer, serous cystadenoma, pancreatic intraepithelial neoplasia (PanIN) 1-2, villous adenoma and gastrointestinal stromal tumor (GIST).

3.8 POSTOPERATIVE COMPLICATIONS – PANCREATIC FISTULA

In Study IV, the estimated PRV and PDW were correlated to the postoperative outcome and specifically to the development of pancreatic leakage and fistula formation (PF), as this is defined in the introduction section. In the same study, the modified Clavien-Dindo scoring system [99] was used for the classification of the overall postoperative morbidity.

3.9 RADIATION DOSE MEASUREMENTS

In Studies I and III, the estimated radiation dose was used for comparison, due to the fact that the scanner's tube voltage varied between the compared protocols.
In Study I, the volume CT dose index (CTDIvol) was measured by using a pencil ionization chamber (DCT10, Wellhöfer, Germany) inside a 32 cm body phantom. The results are presented in Table 5.
In Study III, the CTDIvol and dose length product (DLP) were provided by the CT scanner. The effective dose (ED) was estimated by multiplying the DLP by a conversion factor of 0.0153 for 120 kV examinations and 0.0151 for the 80 kV examinations [100]. The results are presented in the results section.

3.10 STATISTICAL ANALYSES

Study I

DBM-MRMC software version 2.2 was used for the statistical analysis [101]. The study was analyzed using the receiver operation characteristic (ROC) method and calculating a figure of merit (FOM) for each reader and protocol [102]. Multiple comparisons of continuous data were performed by analysis of variance (ANOVA). In the case of a statistically significant result, statistical comparisons were made by using the post-hoc test to control for multiplicity as proposed by Fisher. Because the ROC methodology cannot handle information about the number of lesions per case and their localization, the lesion localization fraction (LLF) and the non-lesion localization fraction (NLF) were calculated using the formulas:

i) LLF=LL/n, whereby LL is the lesion localization defined as a mark no more than 1 cm from the lesion and n is the total number of lesions, and

ii) NLF=NL/n, whereby NL is the non-lesion localization defined as a mark located more than 1 cm from a lesion and n is the total number of cases.

Study II

For the interobserver agreement, the intraclass correlation coefficient (ICC) was calculated according to the method presented and described by Shrout & Fleiss [103] and Bland & Altman [104]. A score between 0–0.2 indicates poor agreement, 0.3–0.4 indicates fair, 0.5–0.6 indicates moderate, 0.7–0.8 indicates strong and more than 0.8 indicates a very strong and almost perfect agreement. The correlation between the imaging assessment and the surgical outcome, R0 rate and median survival was done with descriptive statistics.

Study III

SAS version 9.4 (SAS Institute Inc., Cary, NC, USA) was used for the statistical analysis. ANOVA and post-hoc analysis (t-test) were performed as described in Study I. In order to evaluate hypotheses of variables in contingency tables, the Chi-square test was used or, in the case of small expected frequencies, Fisher's exact test. The Pearson correlation coefficient was used in order to test independence between variables. In addition to that, descriptive statistics were used to characterize the data.

Study IV

The statistical analysis was performed using SPSS 19.0 software (SPSS Inc., Chicago, IL, USA). All tests of statistical significance were two-sided. Pearson’s Chi-square and the Spearman correlation test were used for categorical values. Logistic regression analyses were performed to identify risk factors for pancreatic fistulae, with and without simultaneous adjustment for competing risk factors. Crude associations were studied in a univariate model, which was followed by a multivariate analysis of the respective factors.

4 RESULTS

4.1 STUDY I

The highest reader-averaged FOM was acquired for PC using a free-choice window setting. The lowest reader-averaged FOM was acquired for PA, using a free-choice window setting. The FOMs for each reader and protocol are presented in Table 7.

Table 7. FOMs for each reader and protocol and the reader-averaged FOM

	Protocols					
	120 kV	80 kV		120 kV	80 kV	
	PA	PB	PC	PA*	PB*	PC*
Reader 1	0.720	0.785	0.840	0.706	0.771	0.833
Reader 2	0.741	0.795	0.836	0.704	0.807	0.842
Reader 3	0.679	0.829	0.834	0.716	0.842	0.876
Average	0.713	0.803	0.837	0.709	0.807	0.850

* free window setting; FOM: figure of merit; PA: protocol A; PB: protocol B; PC: protocol C.

The reader-averaged FOM differed significantly (P<0.0001), which means that at least two protocols differed. The results of the post-hoc analysis are presented in Table 8.

Table 8. Inter-protocol comparison

Protocol comparison	**Δ FOM**	**P-value**
C* - A*	0.1419	<0.0001
C* - A	0.1372	<0.0001
C - A*	0.1283	<0.0001
C - A	0.1237	<0.0001
B* - A*	0.0979	0.0003
B - A*	0.0943	0.0005
B* - A	0.0933	0.0006
B - A	0.0897	0.0010
C* - B	0.0475	0.0797
C* - B*	0.0439	0.1053
C - B	0.0340	0.2097
C - B*	0.0304	0.2621
C* - C	0.0135	0.6174
A - A*	0.0046	0.8644
B* - B	0.0036	0.8941

*: free window setting; Δ FOM: differences between the figures of merit.

Tumor detection was significantly better with the 80 kV protocols (PB and PC) compared with the 120 kV protocol (PA). No significant difference was obtained between the two 80 kV protocols or between the fixed and the free window setting.

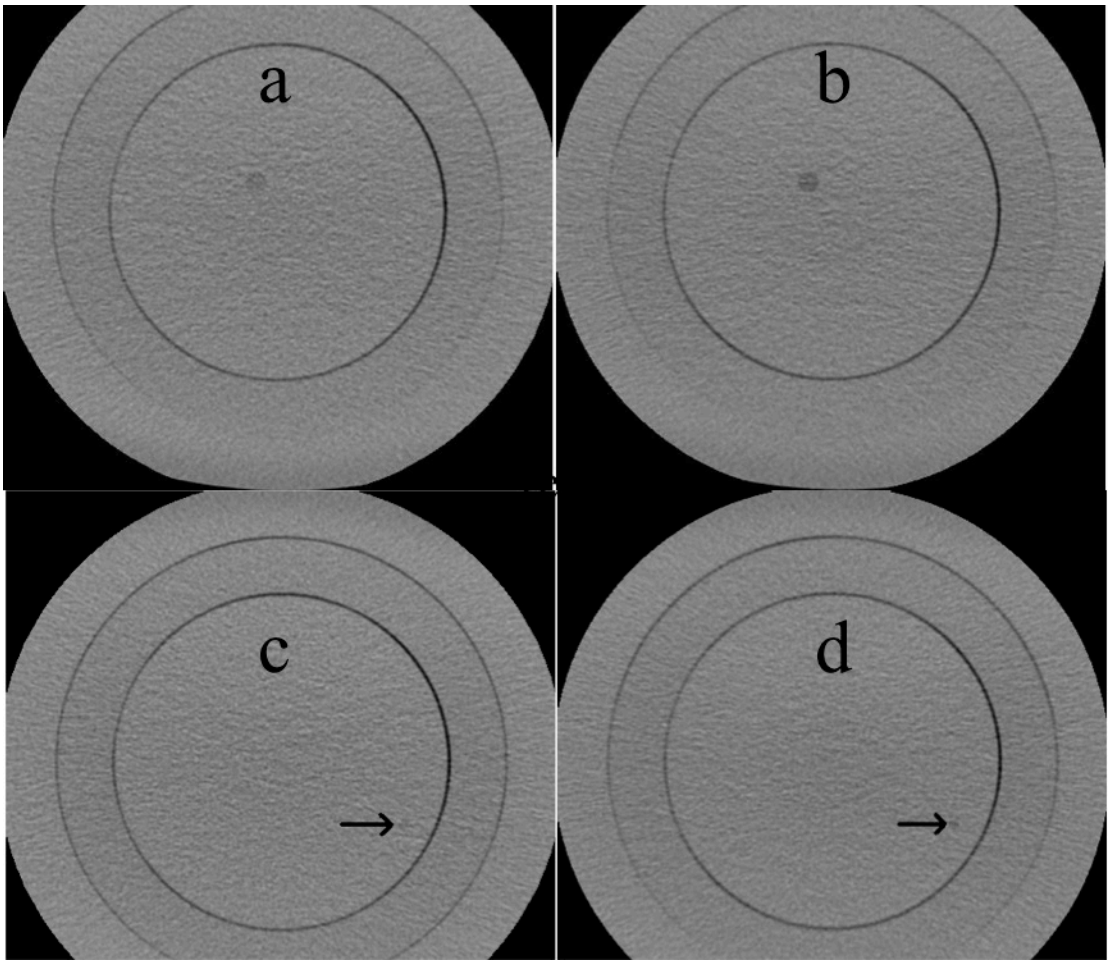

Figure 4. Images of the phantom scanned at 120 kV (a, c) and 80 kV (b, d) with the same image noise. Images (a) and (b) depict a 10 mm lesion and images (c) and (d), a 5 mm lesion (black arrow). The 10 mm lesion is visualized in both protocols. However, the parenchyma-to-lesion attenuation difference is higher and the subjective lesion delineation is better at 80 kV (b). The 5 mm lesion can hardly be delineated at 120 kV (c).

For the descriptive statistics the LLF is presented in Figure 5.

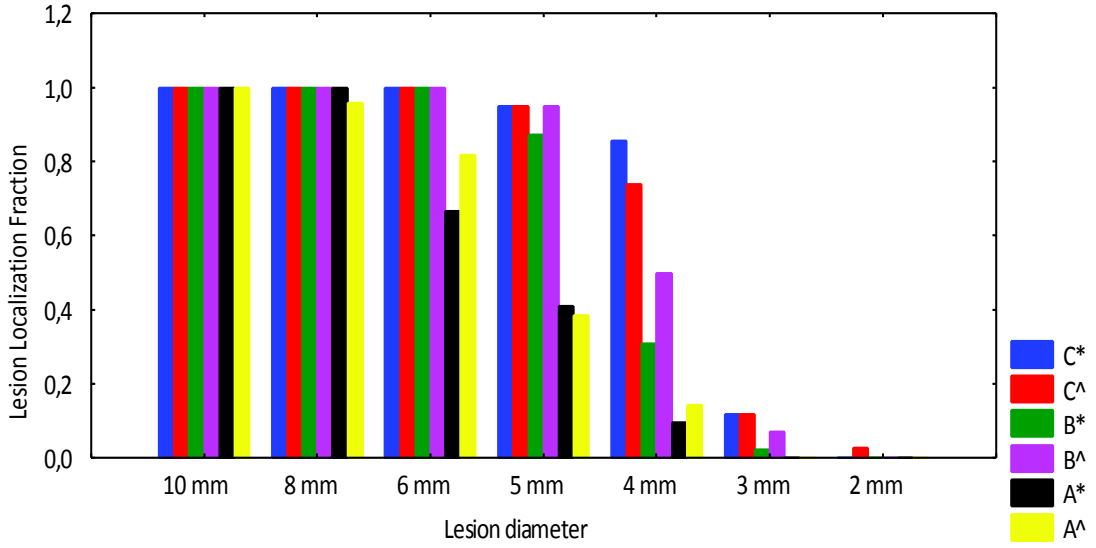

Figure 5: The reader-averaged lesion localization fraction (LLF) for each lesion size and protocol (*: free window setting; ^: fixed window setting; C: protocol C; B: protocol B; A: protocol A)

The bar graphs in Figure 5 show that all protocols are good and equal for detecting lesions 8 and 10 mm in diameter. The 80kV protocols are superior to the 120kV protocol for detecting 5 and 6 mm lesions. For lesions smaller than 5 mm, no protocol revealed satisfactory results.

4.2 STUDY II

The overall ICC showed almost perfect agreement between radiologists with different levels of expertise in local vessel assessment in patients with PDAC in the head of the pancreas. Results are presented in Table 9.

Table 9. The interobserver variability for each reader group and overall

Group	**ICC**
Trainees	0.846
Experienced	0.759
Experts	0.919
Overall	0.94

ICC: intraclass correlation coefficient.

In 22 of the 30 patients, six or more readers classified the tumor in the same category. In the remaining 8 patients, consensus was obtained between three readers (one from each level of expertise). The distribution of the vascular resection in the different categories is presented in Table 10.

Table 10. Radiological staging as related to subsequent vascular resection

Category	Number of patients	Surgical report				
		No vessel resection	Vein resection	Artery resection	Artery + vein resection	Unresectable
A1	9	9				
A2	10	6	4			
B1	0					
B2	2	1	1			
C	3	1	2			
D	6		2	1	1	2

In all nine tumors classified as category A1 no sign of vascular invasion was observed during surgery. In 40% of tumors classified as category A2 (4/10), a corresponding infiltration of the SMV/PV was observed and a resection of the respective vessel was found to be necessary. In category B2, one of the two tumors (50%) required SMV/PV resection. Two out of three tumors (67%) in category C had corresponding vein resections. All six patients with tumors classified as category D had signs of vascular involvement during surgical exploration. Two of them (33%) had a locally advanced tumor deemed to be unresectable.

Finally, the R0 rate was 33%, 25% and 0% in group 1, 2 and 3, respectively. The median survival was 20, 22 and 12 months in group 1, 2 and 3, respectively.

4.3 STUDY III

Significantly better tumor delineation (clear - sharp) in PD (86%) and PE (87.5%) compared to PS (65%) (*P*=0.02). Results are presented in Table 11.
In two patients, one of the readers deemed the tumor not visible in PS and poorly or clearly visible with PE and PD, respectively (Figure 6). At 80 kV, all tumors were deemed as visible.

Table 11. Comparison of the parameter "tumor delineation" between the three protocols (PS, PD and PE) for each reader and overall

	PS		PD		PE		*P*-value
	None/ poor	Clear/ sharp	None/ poor	Clear/ sharp	None/ poor	Clear/ sharp	
Reader 1	7/30 23%	23/30 77%	2/14 14%	12/14 86%	3/16 19%	13/16 81%	0.7
Reader 2	14/30 47%	16/30 53%	2/14 14%	12/14 86%	1/16 6%	15/16 94%	0.006
Overall	21/60 35%	39/60 65%	4/28 14%	24/28 86%	4/32 13%	28/32 87%	0.02[1]

[1]PS vs. PD: *P*=0.04; PS vs. PE: *P*=0.02; PD vs. PE: *P*=0.8. PS: standard protocol; PD: protocol D; PE: protocol E.

Figure 6. Coronal MDCT images of a patient with ductal adenocarcinoma in the head of the pancreas (open arrow) during the pancreatic parenchymal (a, b) and portal venous (c, d) imaging phases. Images (a) and (c) were obtained at 80 kV (normal iodine-load; protocol D) whereas (b) and (d) were obtained at 120 kV (PS). For both readers, delineation of the tumor was clear with PD and poor or absent with PS, respectively. Superior opacification of mesenteric branches (arrowheads) during both imaging phases in the 80 kV (a, c) compared to the 120 kV examinations (b, d) may also be observed. A common bile duct stent is indicated by the black arrow.

No significant difference was observed between the three protocols regarding assessment of vessel involvement. For Readers 1 and 2, the accuracy of PS, PD and PE for vessel assessment was 95/91%, 92/94%, and 92/90%, respectively.
All three protocols resulted in a slight overestimation of HA involvement (Figure 7). In four patients (one from Reader 1, two from Reader 2 and one from both readers), the HA was assessed as encased with PS. In only one patient, a short segment of HA was resected and perivascular tumor infiltration was observed microscopically. In one patient using PD (both readers) and one using PE (Reader 2), the HA was assessed as encased but none of these patients required a HA resection.

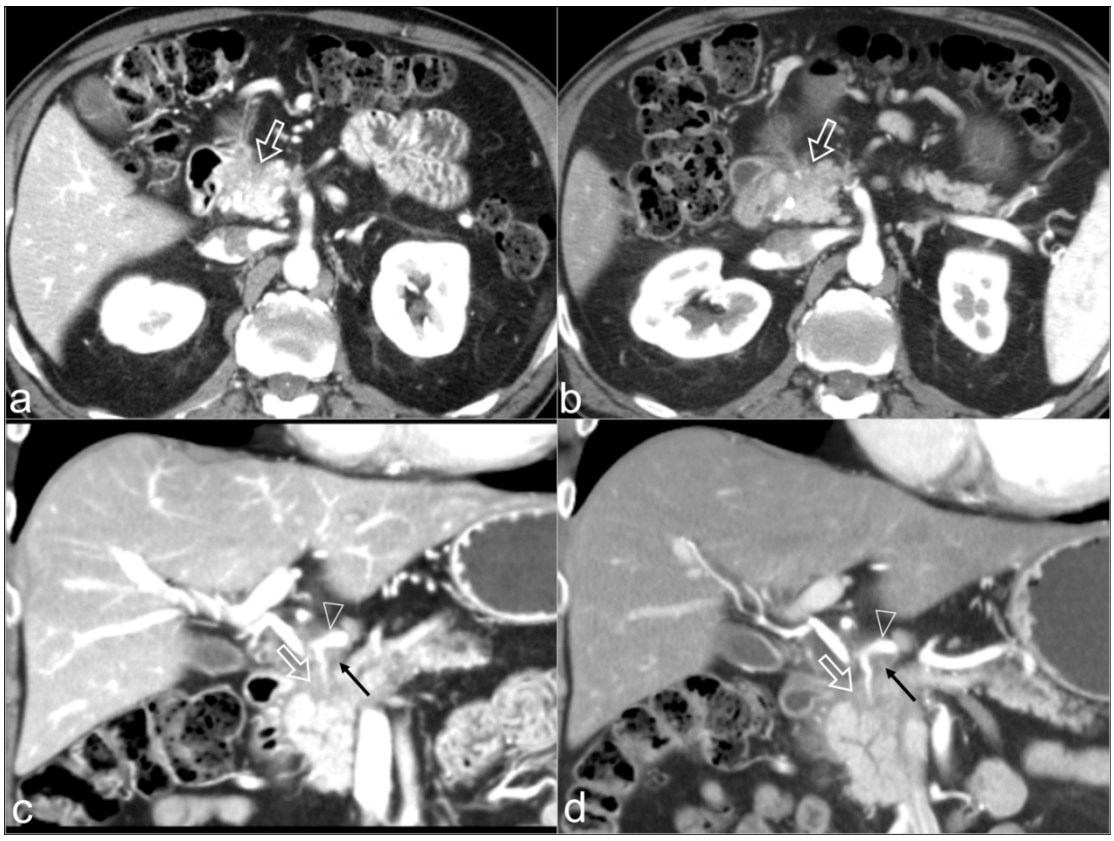

Figure 7: Axial (a, b) and coronal (c, d) MDCT images of a patient with ductal adenocarcinoma in the head of the pancreas (open white arrow) during PPP. Images (a) and (c) were obtained with PD whereas (b) and (d) were taken with PS. Both readers assigned hepatic artery (HA) encasement (arrowhead) by the tumor at the origin of the gastroduodenal artery (black arrow) in both examinations. During surgery, no signs of infiltration of the HA were present.

No significant difference was found between the protocols in both PPP and PVP in image quality. PPP in PS, PD, and PE was graded as excellent in 87%, 79%, and 69% of cases, respectively. The rest of the cases were graded as good. Image quality was not graded as poor or acceptable in any of the cases. PVP in PS, PD, and PE was graded as excellent in 78%, 50%, and 58% of cases, respectively. In each protocol, PD and PE, one case was graded as acceptable (4%). The rest of the cases were graded as good.

The pancreatic parenchymal/tumor attenuation, parenchyma-to-tumor attenuation difference as well as the parenchyma-to-tumor CNR and FOM are presented in Table 12.

Table 12. Comparison between the three protocols (PS, PD and PE) for the parameters parenchyma-tumor attenuation, parenchyma-tumor attenuation difference, parenchyma-to-tumor CNR and FOM

	PS	PD	PE	*P*-value		
				PS vs PD	PS vs PE	PD vs PE
PPP (SD)						
Parenchyma HU	150 (29)	232 (47)	298 (55)	<0.0001	<0.0001	<0.0001
Tumor HU	90 (24)	125 (23)	140 (47)	<0.0001	<0.0001	0.26
Attenuation difference HU	59 (28)	89 (45)	158 (72)	0.01	<0.0001	0.005
CNR	8 (4)	9 (5)	15 (8)	0.34	0.0002	0.02
FOM	6 (6)	11 (9)	36 (41)	0.03	0.002	0.03
PVP (SD)						
Parenchyma HU	116 (16)	180 (35)	231 (28)	<0.0001	<0.0001	0.0008
Tumor HU	86 (18)	121 (38)	145 (40)	0.0002	<0.0001	0.14
Attenuation difference HU	30 (21)	60 (36)	85 (47)	0.002	<0.0001	0.15
CNR	3 (2)	4 (3)	5 (4)	0.05	0.003	0.4
FOM	2 (3)	5 (6)	7 (10)	0.03	0.01	0.5

SD: standard deviation; PPP: pancreatic parenchymal phase; PVP: portal venous phase; CNR: parenchyma-to-tumor contrast-to-noise ratio; FOM: figure of merit.

In both imaging phases, pancreatic parenchymal attenuation was highest in PE and the difference from PD and PS was statistically significant. The measurements of tumor attenuation in the two imaging phases were comparable for all three protocols. In PPP, the parenchyma-to-tumor attenuation difference and parenchyma-to-tumor CNR were significantly higher in PE compared to PD and PS. In the same phase, i.e. PPP, the normalized parenchyma-to-tumor CNR as expressed by FOM was significantly higher in PE and PD as compared to PS.

The mean parenchyma-to-tumor attenuation difference in PE in PVP is similar to attenuation difference in PD in PPP and higher than the attenuation difference in PS in PPP.

The radiation dose was significantly higher for PS compared to PD and PE. The mean CTDIvol, mean DLP and mean ED for all the protocols (for both PPP and PVP) are described in Table 13.

Table 13. Comparison between the three protocols (PS, PD and PE) for radiation dose parameters

	PS	PD	PE	*P*-value
CTDIvol, in mGy (SD)	52 (18)	35 (10)	34 (10)	[1,2] 0.003 [3] 0.9
DLP, in mGy x mm (SD)	1660 (626)	1160 (426)	1100 (318)	[1] 0.02 [2] 0.006 [3] 0.7
ED, in mSv (SD)	25 (9)	18 (6)	17 (5)	[1] 0.01 [2] 0.004 [3] 0.7

[1]: PS vs. PD. [2]: PS vs. PE. [3]: PD vs. PE. CTDIvol: computed tomography dose index dose index; DPL: dose length product; ED: effective dose; SD: standard deviation

4.4 STUDY IV

In total 120 patients (66%) out of the 182 experienced postoperative complications (Clavien >1) and 31 (17%) of them had a severe complication (Clavien ≥ 3b). The most common complication was PF. All the postoperative complications are described in Table 14.

Table 14. Postoperative complications and pancreatic fistula formation (PF) after pancreaticoduodenectomy

Complication	Number of patients (%)
Pancreatic fistula	38 (20.9)
Grade A	3 (1.6)
Grade B	21 (11.5)
Grade C	14 (7.7)
Abscess	24 (13.2) 8 without PF
Intra-abdominal bleeding	13 (7.1) 5 without PF
GI bleeding	6 (3.1) 5 without PF
Delayed gastric emptying	16 (8.8) 14 without PF
Bile leakage	8 (4.4) 5 without PF
Lymph leakage	6 (3.3) 6 without PF
Sepsis	4 (2.2) 2 without PF
Pulmonary embolism	3 (1.7) 3 without PF
Reoperation	24 (13.2) 13 without PF
Death	3 (1,6) 1 without PF

The mean PRV was 36.9 (SD=15.5) cm^3 (Figure 8). The mean PDW was 4.6 (SD=3.0) mm (Figure 9). Corresponding values at the 25^{th}, median, and 75^{th} percentiles were 24.9, 35.2, and 46.7 cm^3 for PRV and 2.1, 3.9, 7.1 mm for PDW, respectively. No patient with PRV at the 1^{st} quartile developed a clinically significant PF (grade B or C). Only one patient with PDW in the 75^{th} quartile developed PF.

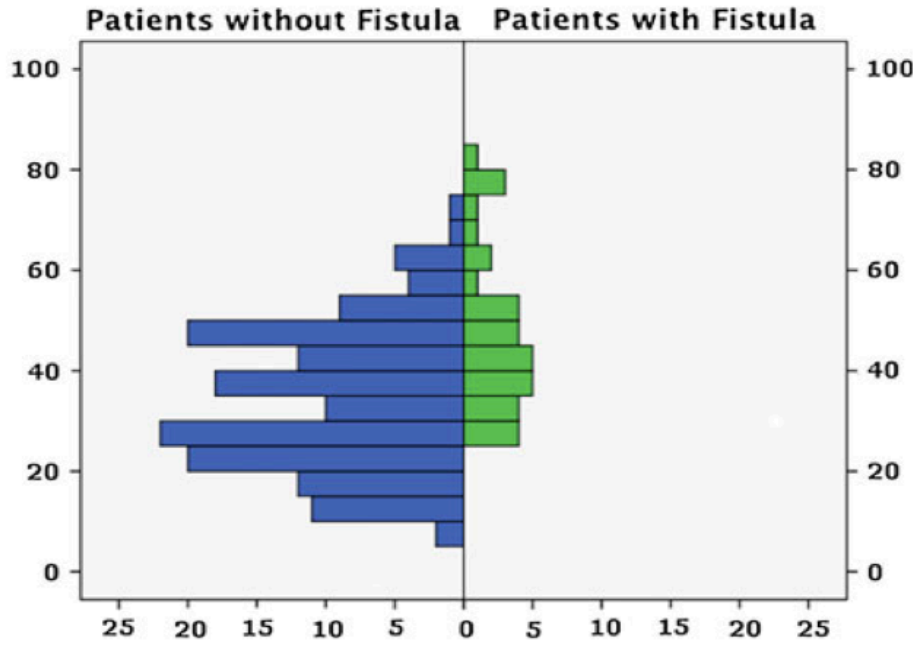

Figure 8: Distribution of pancreatic remnant volume (cm^3) in patients with or without grade B and C fistula.

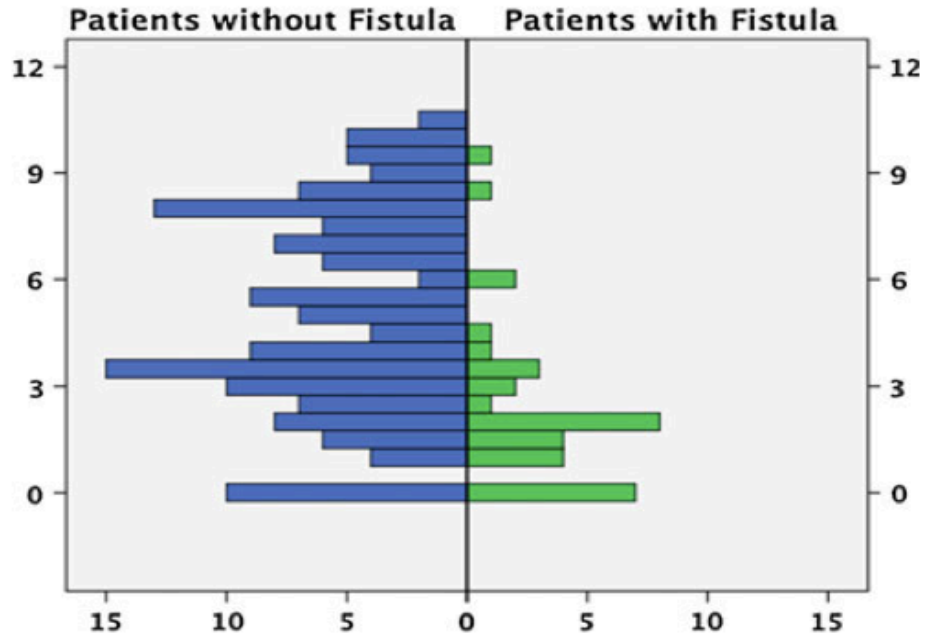

Figure 9: Distribution of pancreatic duct width (mm) in patients with or without grade B and C fistula.

Logistic regression analyses were performed to identify potential determinant variables (Table 15). In the multivariate analyses, a large PRV or small PDW significantly increases the risk for PF, independently.

Table 15. Univariate and multivariate analyses of risk factors for grade B and C PF

Variable	**Number of PF (%)**	**Univariate analysis**			**Multivariate analysis**		
		OR	95%CI	P value	OR	95%CI	P value
[1]PRV-cm^3							
<35.2	8/75(9.4)	1	1.58-8.71	<0.01	1	1.27-6.27	<0.01
≥35.2	27/97 (27.8)	3.71			2.55		
PDW-mm							
<3.9	30/91 (33.3)	8.46	3.11-23.04	<0.01	6.94	2.51-19.23	<0.01
≥3.9	5/91 (5.5)	1			1		
Female	11/88 (11.4)	0.49	0.27-1.05	0.07			
Male	22/94 (23.4)	1					
Diabetes	2/26 (7.7)	0.35	0.078-1.56	0.17			
BMI 20-30	29/152	1	1	0.58			
BMI >30	2/16 (18.8)	0.65	0.140-3.0	0.31			
BMI <20	1/14 (7.1)	0.34	0.04-2.7				
Malignant	23/144 (16.0)	0.61	0.26-1.46	0.27			
Benign	9/38 (23.7)	1	1				
R1-resection	11/77 (14.3)	0.67	0.30-1.48	0.32			

[1]: Cutoff at the median value. PF: pancreatic fistula; PRV: pancreatic remnant volume; PDW: pancreatic duct width; BMI: body mass index; OR: odds ratio; CI: confidence interval.

5 DISCUSSION

This thesis was intended to evaluate the role of 64-channel MDCT on pancreatic cancer diagnosis (Studies I and III), local staging assessment (Studies II and III) and prediction of postoperative complications (Study IV). More specifically, the roles of the current institutional standard examination protocol (Studies I, II and III) and classification system (Study II) were investigated. Additionally an attempt to improve tumor diagnosis (Studies I and III) and local staging assessment (Study III) was made by first using an experimental model (Study I) and afterwards conducting a prospective randomized clinical study (Study III), in order to study the effect of lowering the tube-voltage and increasing the iodine-load.

5.1 DIAGNOSIS

The late arterial phase or so-called pancreatic parenchymal phase is well known as the optimal phase in which to detect and delineate the majority of pancreatic cancers. The rationale behind this is the higher attenuation difference between the hypovascularized fibrotic tumor and the avidly enhanced normal pancreatic parenchyma compared to the other scanning phases. The reasoning for using a low-tube-voltage protocol was to study whether tumor conspicuity can be improved by achieving a higher attenuation difference between the simulated digital lesions and the background for Study I, and between the tumor and the normal pancreatic parenchyma for Study III. When the tube voltage is decreased from 120 kV to 80 kV, the mean photon energy decreases in parallel from 56.8 to 43.7 keV [78] which is closer to the K edge of iodine (33.2 keV) resulting in higher X-ray absorption and a significantly higher attenuation of iodine-containing tissues. Consequently, the attenuation difference between the simulated lesions and the background – Study I – and between the tumors and the pancreatic parenchyma – Study III – increases by 70% (from 20 HU to 34 HU) and 51% (from 59 HU to 89 HU), respectively. However, the increase in attenuation difference in Study III becomes even higher (168%) when both low tube-voltage and high iodine-load are combined. Even though the attenuation of both parenchyma and lesion increases gradually between normal-tube-voltage, low-tube-voltage and low-tube-voltage high-iodine-load protocols, respectively, the relative increase of the parenchymal attenuation is predominant, which results in a significantly higher attenuation difference.

The results of the phantom Study I showed the superiority of low-tube-voltage protocols regarding the detection of small hypoattenuating tumors. It has been revealed that both low-tube-voltage and normal-tube-voltage protocols are equal and adequate for detecting lesions 8 and 10 mm in diameter in an optimal experimental environment. However, smaller lesions (5-6 mm) are easily missed with the normal-tube-voltage protocol but may be detected by decreasing the scanner's tube voltage.

The results of the randomized prospective Study III showed the superiority of a low-tube-voltage high-iodine-load MDCT protocol regarding tumor conspicuity in

patients with pancreatic cancer. The tumor's borders become sharper as the image contrast decreases and, despite the increase in image noise, image quality is not compromised. Even though the subjective evaluation of tumor conspicuity yielded no significant difference between the low-tube-voltage normal-iodine-load and low-tube-voltage high-iodine-load protocols, the objective attenuation difference expressed in terms of CNR and FOM, is higher when a combination of both parameters is applied.

An interesting and unexpected finding was the higher parenchyma-to-tumor attenuation difference in PVP of the low-tube-voltage high-iodine-load protocol (PE) (85 ± 47, mean ± SD) compared to PPP of the normal-tube-voltage normal-iodine-load protocol (PS) (59 ± 28, mean ± SD). The clinical implication of this result is that the PVP obtained with the optimized protocol could eventually replace the PPP. In that way, both the examination time and the radiation dose can be decreased.

5.2 LOCAL STAGING

Staging of patients with pancreatic cancer using MDCT is central to their clinical management. Based on the fact that surgery with or without radiochemotherapy is the only curative treatment for PDAC, it is critical that the preoperative radiological examinations provide accurate information in order to reach the optimal therapeutic decision for the individual patient.

The results of Study II showed strong agreement between radiologists regardless of their level of expertise in assessing the tumor involvement of the major peripancreatic vessels using our institution's MDCT standard examination protocol (120 kV and 0.75 g I/kg) and based on our hospital's classification system (A1 to D). Although a slight variation was seen in the ICC values between the three groups of radiologists, trainees, experienced and experts (ICC values of 0.85, 0.76, and 0.92 respectively), this was not deemed clinically significant.

The second major finding of Study II showed that as the classification goes from A1 to D (in practical terms translating into progression of the local tumor stage), the degree of vascular involvement and the probability of en-bloc vascular resection or surgical unresectability increase. In this context, a subgrouping of the A and B categories (Table 4) is proposed based on the assumption that these categories lead to important alterations in the planning of a therapeutic strategy. Recently, there has been an attempt to divide category D into D1 and D2, distinguishing those patients who have a technically resectable tumor (D1 i.e. no engagement of the mesenteric branching or hepatic artery bifurcation) and may benefit from neoadjuvant treatment from those that do not (D2). Further prospective studies are needed to investigate the potential impact of this differentiation on patients' short- and long-term survival.

At a first glance, this classification system may look complex, consisting of different interconnecting elements. However, the objective is to reflect reality and basically

cover the clinically relevant combinations of venous and/or arterial involvements. Each vessel is evaluated separately and when this assessment is completed, each patient is placed in the respective category (from A1 to D). Furthermore, the results from younger, less experienced radiologists suggest that our classification system is easy to learn and use.

The definition of surgical resectability of PDAC has changed in recent decades. This is mainly due to the introduction of new, more aggressive surgical techniques allowing vessel resection and reconstruction (i.e. resection of the mesenterico-portal axis or short-segment resection of the HA as well as CA resection in distal tumors). However, the classification system proposed by Lu [58], which takes into consideration the circumference of the vessel that is contiguous to the tumor, remains the cornerstone of the most widely used and accepted classification systems for the assessment of the main peripancreatic vascular involvement. In Study III, we chose to correlate the assessment of vascular involvement to the surgical and histopathological outcome based on Lu's classification and not to our department's classification system as in Study II, for two reasons. First, our department's classification (A1 to D) reflects a probability for vascular resection in each group, which make it impossible to compare the radiological imaging findings with the actual vascular status (gold standard). Second, our classification system was developed for tumors located in the head of the pancreas, whereas in Study III patients with distal tumors were also included.

The results of Study III showed similar vessel involvement assessment between normal tube-voltage and low-tube-voltage with or without high-iodine-load protocols. One interesting finding from this study is the overestimation of the extent of arterial involvement, predominantly of the HA, a finding which corresponds with the results from another recent study [19]. This is the reason why the International Study Group of Pancreatic Surgery recommends surgical exploration in cases where the HA appears encased on preoperative imaging [42].

In Study III, two patients showed histopathological signs of periarterial tissue infiltration (HA and CA respectively). Arterial wall involvement is rarely observed due to the rigidity of the arterial wall compared to the venous, while perivascular infiltration is more common. Surgical resection is, however, warranted in both instances. For that reason, both vessels were considered as infiltrated in the imaging analysis.

In Studies II and III, the population was limited to patients diagnosed with potentially resectable PDAC undergoing surgery with curative intent. Our intent was to investigate tumor resectability as we did not consider the investigation of tumor unresectability relevant due to the results of previous studies that showed a PPV as high as 100%. Moreover, in order to correlate the preoperative vascular involvement assessment with the surgical and histopathological outcome, surgical exploration was mandatory. However, this choice can lead to a selection bias with the risk of overestimating the

accuracy of all MDCT protocols regarding the assessment of vessel engagement because the anticipated extent of the vascular involvement in our series was much lower compared to that of the unselected cohort of patients with PDAC. The evaluation of the vascular involvement in patients belonging to more advanced categories/stages, and specifically the interobserver variability assessment, is the subject of an ongoing study at our institution.

Neoadjuvant therapy can potentially alter the radiological evaluation. A recent study showed that classical resectability criteria could not be used in this group of patients [105]. Hence, we excluded all those patients receiving any kind of neoadjuvant therapy from all the clinical studies (Studies II, III and IV).

5.3 PREDICTION OF POSTOPERATIVE COMPLICATIONS

The results of Study IV showed that high PRV and/or small PDW at the transection line after PDE are significantly and independently correlated with a high risk of postoperative PF. The association between the preoperative estimated PRV/PDW and the incidence of non-clinically significant grade A PF as well as clinically significant grade B and C was observed.

Obviously, the PF rate and morbidity in general are substantial after PDE, as seen in this series, as well as in many other recent reports from high-volume centers [106]. It is also evident, although complication rates are high, that these complications can be managed successfully with low in-hospital mortality and a decent length of hospital stay. Two main theories underlie the findings of Study IV. First, while the normal pancreatic tissue is being replaced by fibrosis, the volume decreases and the duct diameter increases [107]. A recent study from our institution revealed a close relationship between the preoperative PRV and PDW estimation and the related intraoperative assessment of the gland texture and PDW in predicting postoperative PF [108]. Second, the larger the gland the more digestive juice produced per unit time and this compromises the healing of the pancreatico-enteric anastomosis.

5.4 TECHNICAL CONSIDERATIONS

Our main consideration by decreasing the tube voltage in both Studies I and III is the increase of image noise. To overcome and test this potential limitation in Study I, in one of the two low-tube-voltage protocols (PC), we maximized the tube current (675 mA) in order to achieve equivalent image noise as in the normal-tube-voltage protocol (PA). The results revealed no significant difference in tumor detection between the two low-tube-voltage protocols. In Study III, even though the radiation dose was decreased in the low-tube-voltage protocols, despite the higher tube-current, and the image noise was increased, the image quality was not compromised.

Increasing the scanner's tube current consequently increases the radiation dose to the patient. The risk of developing a radiation-induced cancer is markedly age-dependent. The median age of PDAC diagnosis is 71 years and the overall 5-year survival rate is less than 5% [109]. If we take these facts into consideration, the risk for this group of patients of developing a radiation-induced cancer as a result of a MDCT-related increase in radiation dose is essentially negligible. However, there is a group of healthy individuals with either predisposing or genetic factors associated with increased risk for PDAC that undergoes screening routinely. The radiation dose should be taken into account in these patients and new, simplified but high specificity techniques should be developed. At our institution there has been an attempt to shorten the CT examination protocol for these patients by scanning the pancreas only in the PPP.

In our standard institutional MDCT protocol we use 0.75 g I/kg body-weight, which has been shown to be superior to lesser iodine dosage levels in liver and pancreatic imaging [89]. In protocol PE, further increasing the iodine load to 1 g I/kg body-weight was found to be of great clinical benefit. To the best of our knowledge, there are no previous studies testing such a high dosage of CM.

In Study I, two of the three readers did not generate an appreciable amount of NLs for the 80kV protocols with the free-window setting and thus the statistical analysis became less reliable. For that reason a ROC analysis was performed even though the initial study design was based on free-response ROC (FROC). The highest rated mark per case was used for the ROC evaluation. Complementary descriptive statistics were done so that the information about the location and the number of lesions was not lost. The ROC methodology is considered very powerful because it estimates and reports all combinations of sensitivity and specificity that a diagnostic test is able to provide [110].

In both Studies II and III, the scanner's tube current was set by automatic tube current modulation (ATCM). The ATCM technique combined with a proper noise index to maintain an adequate image quality has the potential to reduce the total radiation dose level [40]. The maximum level was set at 800 mA and 675 mA for the 120 kV and 80 kV protocols, respectively, which represents the maximum tube current that our 64-channel MDCT can generate in the respective tube voltage levels.

5.5 LIMITATIONS

Study I

The ideal spherical shape of a tumor in the ideal homogenous background does not reflect daily clinical practice. PDAC is an infiltrative, fibrotic tumor that sometimes hardly delineates from the normal pancreatic parenchyma and peripancreatic tissues. Furthermore, approximately one out of 10 tumors is isoattenuating compared to the normal pancreatic parenchyma even in the PPP. The attenuation used as a reference in Study I for pancreatic parenchyma (130 HU) and pancreatic cancer (110 HU) at 120 kV was measured in a limited number of patients (n=15). However, in Study III the mean

attenuation of the pancreatic parenchyma and pancreatic cancer in PPP at the same tube voltage were 149 HU and 90 HU respectively and the mean attenuation difference was 59 HU. These results show that the mean parenchymal attenuation measured in a larger group of patients (n=30) was close to that chosen for Study I. On the other hand, the mean attenuation of the tumor and the mean pancreas-to-tumor attenuation difference were lower and higher, respectively, revealing that the Study I hypothesis reflects only a few cases in clinical practice, quite close to the "worst case scenario", i.e. tumors that have attenuation similar to the parenchyma.

Technical issues concerning the CT scan and image processing are some further limitations of this study. Overweight/obese patients are not suitable for 80 kV MDCT because of the high image noise which cannot be optimally compensated for by the maximal increase in the radiation dose. Furthermore, the simulated tumors were inserted into reconstructed images, meaning that the lesions were not affected by the modular transfer function (MTF) of the system. In future studies, the lesions may instead be convolved with the point-spread function (PSF) before inserting them into the images in order to avoid this inconsistency.

Study II

One major limitation of Study II is the limited number of cases in some groups and subgroups. In our attempt to have the most homogenous study material possible, with all examinations being state-of-the-art, only 30 patients were eligible for inclusion. Indeed, category B1 (SMV/PV involvement >180° and ≤ 2 cm) does not contain a single patient. Moreover, only three of the 30 patients (10%) were classified as category C following the consensus image reading. There were also only a few patients classified as category D. Additionally, due to the small sample size, statistical comparison between the different categories and the outcome could not be performed. Therefore further studies with larger patient populations, including a substantial number of patients with locally advanced tumors, are needed to determine the relevancy of this subgrouping and the applicability of this classification system for more locally advanced disease.

Another potential limitation is that the present classification system was based entirely on the relationship between the tumor and the adjacent major peripancreatic vessels, in the absence of distant metastasis or peritoneal spread. This does not mean that the tumor's relationship to the remaining three-dimensional anatomical structures in the area is prognostically or therapeutically irrelevant. Future studies, especially when combined with dedicated, highly specialized pathology reporting, must address these issues and their clinical significance. Based on the results of such studies, further refinement and adjustments of the present PDAC classification system might be required. However, tumor resection with negative resection margins as an indicator of curative surgery is possible even in cases where adjacent organs, such as the stomach and/or colon are infiltrated.

Furthermore, concerns could be potentially raised about the CT technique used during the study period between October 2006 and December 2010 and the possibility of using a more recent patient group in order to have CT examinations of higher quality due to the rapidly evolving MDCT technology. As stated in the methods section, all patients were examined with the same 64-channel MDCT scanner using the same examination protocol, which is the standard protocol currently used in our department. However, bearing in mind the results of Study III, new, larger, prospective, well-designed studies should be conducted in order to correlate this classification system to surgery in CT examinations obtained with the optimized low-tube-voltage high-iodine-load protocol.

Study III

A potential limitation of our study is the fact that in nine patients there was a slight variation in the rotation time during the acquisition of PPP at 80 kV (1 second instead of the predetermined level of 0.6 seconds), which is a potentially important technical parameter. By increasing the rotation time the radiation dose increases and the image noise decreases, which may lead to an overestimation of tumor conspicuity during those 80 kV examinations. We decided, however, to include data from these nine patients because comparing the CDTIvol between the 80 and 120 kV examinations, it was shown that the radiation dose level of the 80 kV examinations did not reach the dose level of 120 kV, even though the rotation time was 1 second.

Study IV

The preoperative examinations used for volume measurements were those closest to the operation. That led to an inhomogeneous study group with examinations from different institutions, different modalities (CT or MRI) and different acquisition protocols (i.e. variable slice thickness). However, according to Reiner et al. [111] although the mean total liver volume decreases with increased slice thicknesses for both CT and MRI, the difference is not significant if slice thickness is up to 6 mm for CT and 8 mm for MRI. Our protocols were within those limits. In 25 patients those measurements were done by means of MRI images. In 10 of them MDCT examinations were available within a time frame of $\leq$ 1 month and comparison of the volume measurement revealed no statistically significant differences: mean PRV with MDCT 34.4 (SD=10.0) cm^3 and with MRI 33.3 (SD=8.4) cm^3.

It is important to state that in the PRV the volume of the pancreatic duct is included, which may falsely increase the volume of parenchyma. In patients with an atrophic pancreatic parenchyma, a dilated main pancreatic duct often coexists, as both can be consequences of an obstructive expansive process downstream. So the difference between the total PRV and the parenchyma volume after subtraction of the volume of the dilated duct may be large in these patients. From a clinical point of view, measurement of the entire remnant volume is achievable, but additional measurement of the volume from which the duct is deducted would be time-consuming and, thus, hard to pursue in daily clinical practice.

5.6 CLINICAL CONSEQUENCES

In Study I, the main clinical consequence of our findings is that the low-tube-voltage MDCT technique has the potential to improve the detection of smaller PDACs in patients with suspected pancreatic cancer, which may not be visible in the normal-tube-voltage MDCT.

In Study II, one of the main clinical consequences of the findings is that our classification system is potentially a very useful clinical tool. The focus of this classification has been on the main peripancreatic vessels, which are the critical anatomical structures around the pancreatic gland because the involvement of these structures will have immediate consequences for the ensuing therapeutic strategies and surgical planning.

In Study III, the main clinical consequence of our findings, in agreement with the findings of Study I, is the improved tumor conspicuity with the use of the low-tube-voltage MDCT. Moreover, tumor conspicuity can be increased by combining low tube-voltage with high iodine-load.

In Study IV, there are several clinical consequences. First, as it is well known that the surgical outcome is surgeon depended [112], the selection of more skillful and experienced surgeon should be considered, in those cases assessed preoperatively as having a high risk for PF. Second, in certain situations where the risk for postoperative PF formation is high, carrying out a subtotal pancreatectomy may be the wisest option. In doing so, the PF risk decreases while the endocrine function of the gland is preserved, as the distribution of the islet cells is twice as high in the tail of the pancreas as in the head and body [113]. Third, having in mind, which patients are in higher risk for developing PF, can this group of patients be monitored and followed up more closely postoperatively.

6 CONCLUSIONS

The conclusions of this thesis regarding:

1. **Detection:** Normal-tube-voltage 64-chanel MDCT is adequate for detecting tumors of 8 and 10 mm (Study I). However, the detection of smaller tumors can be improved when low-tube-voltage is applied (Study I). Additionally, tumor conspicuity is significantly better when low tube-voltage is combined with high iodine-load (Study III).

2. **Local staging:** The interobserver agreement between radiologists with different expertise levels is almost perfect in assessing the local tumor staging based on the institutional MDCT examination protocol and classification system (Study II). There is a high correlation between the local staging assessment and the surgical outcome based on the same protocol and classification (Study II). Normal-tube-voltage normal-iodine-load protocol is similar to low-tube-voltage with or without high-iodine-load protocol in local resectability assessment (Study III). Slight arterial overestimation may occur with all protocols (Study III).

3. **Prediction:** Preoperative CT and/or MRI, by measuring the PRV and PDW, can predict the risk for the most common and major postoperative complication, which is the PF.

7 FUTURE ASPECTS

Even though the importance of 64-channel MDCT for tumor detection, characterization, staging and prediction of post-operative complications is well-accepted due to its relatively high specificity, sensitivity and high interobserver agreement, there is still potential for further improvement.
Recent revolutionary technological developments in MDCT enabling the use of dual energy (DE) MDCT and perfusion CT offer the possibility to exploit spectral information for diagnostic purposes [114].

Our studies (Studies I and III) have shown that scanning at low tube-voltage improves spatial resolution and image contrast at the expense of image noise. The main principle of DE-MDCT is the acquisition of CT data using two different photon spectra (at 80/100 kV and 140 kV) within a single acquisition. This has the potential to combine the advantages of low and high tube-voltage, which are the increased image contrast and the low image noise, respectively.

Hitherto, many applications of the DE technique have been tested in abdominal imaging and particularly in pancreatic imaging. DE-MDCT energy and perfusion CT are two recent CT techniques for abdominal imaging that may provide additional information about the tissue being examined in combination with the morphological findings [115]. One limitation of single-energy MDCT is the considerable overlap in material attenuation resulting in potential ambiguity for discriminating between different materials [116]. DE-MDCT has the potential to decrease this by interrogating the material-specific attenuation properties at different energy levels [116]. A quite recent study showed that perfusion CT can predict tumor grading, since high grade PDAC has significantly higher peak enhancement intensity and blood volume perfusion parameters [117]. Mileto et al. have recently shown that by using the DE technique, virtual non-contrast images reconstructed from a single-phase contrast enhanced DE-MDCT can replace the conventional NCP with no effect in the image quality. Concurrently the radiation dose is reduced significantly compared to the standard single-energy protocol [118]. Patients with hereditary pancreatic cancer who undergo annual CT examination of the pancreas will certainly benefit from such protocols. Macari et al. have shown that pancreatic tumor conspicuity at 80 kV increases significantly compared with the weighted-average 120kV [119]. However, these observations were done in the portal venous phase and the effect of perfusion CT was not taken into consideration.

Despite the fact that few articles have been published on the impact of DE-MDCT and perfusion CT in pancreatic cancer imaging, further prospective, well-designed clinical trials are needed to investigate the validity of these methods relative to tumor diagnosis, staging and prediction of postoperative complications.

8 ACKNOWLEDGMENTS

All studies were carried out at the Division of Medical Imaging and Technology, Department of Clinical Science, Intervention and Technology (CLINTEC) at Karolinska Institutet, Stockholm, and the Department of Radiology, Karolinska University Hospital, Huddinge.

This thesis would not have been possible without the support of my family, supervisors, mentor, professors, colleagues and friends. I would like to sincerely thank all who have contributed to this work.

I especially want to thank my current main supervisor, **Nikolaos Kartalis**, and my former main supervisor, **Nils Albiin**, for their support, encouragement, excellent guidance and engagement. You have been a great and continuous inspiration for me. I feel so fortunate that I have met such decent and knowledgeable colleagues and friends along my career path.

I also want to thank:

My co-supervisor, Professor **Anders Sundin,** for his wealth of experience and for all the support and help whenever needed.

My co-supervisor, Associate Professor **Ralf Segersvärd,** for his engagement, great knowledge in the field of this thesis and the wise solutions to almost all the problems that we faced during this journey.

My mentor, Professor **Solvig Ekblad,** for our enjoyable meetings at the NK and all the useful advice.

My professor, **Peter Aspelin,** for providing me with the time and an excellent scientific environment for the accomplishment of this thesis.

My professor, colleague and dear friend, **Rimma Axelsson,** for all her invaluable advice and support.

My co-author, **Jon Holm,** for his great contribution to my first paper and for all the time he spent explaining the technical parts of this work to me.

My co-author, colleague, mentor and dear friend, **Bertil Leidner,** for his burning interest in MDCT technology, brilliant ideas and tolerance. He was the first to conceive the idea of pancreatic CT and 80 kV.

My radiologist colleagues and co-authors, **Elisabet Axelsson**, **Aristidis Grigoriadis**, **Michael Fischer** and **Mats Andersson,** for spending their precious time evaluating my

examinations. I would like to express my sincere sympathy to the family of my beloved colleague **Nick Edsborg** who is no longer with us.

My surgeon colleagues and co-authors, **Farshad Frozanpor**, Professor **Lars Lundell**, **Christoph Ansorge** and **Marco Del Chiaro,** for sharing their surgical experience with me and for their contributions towards the writing of my papers.

My pathologist colleague and co-author, **Caroline Verbeke,** for her intelligent contributions to my third paper.

The PhD student **Stefania Marconi** for providing me the image for the cover of this PhD thesis.

The current and former heads of the Department of Radiology at Karolinska University Hospital Huddinge, **Maria Kristoffersen-Wiberg**, **Henry Lindholm** and **Bo Persson,** for providing the time and resources needed for completing this thesis.

Our secretaries, **Helena Forssell** and **Maj-Britt Stäring,** for all the help in dealing with the necessary formalities.

Our assistant nurses, **Ia Wassén** and **Lena Håkansson** for their patience, tolerance and friendliness every time I "demanded" to get my study patients into the CT scanner.

All the **CT technologists** and especially **Nouhad Jallo** and **Anders Svensson**, for their high quality examinations.

Our statistician, **Per Näsman,** for his excellent and time-efficient cooperation.

Our research nurses, **Gunilla Gagnö** and **Birgitta Holmgren,** for their tremendous work maintaining the pancreatic register and including patients in our studies.

I especially want to thank my colleague and dearest friend, **Lena Cavallin,** for listening to all my thoughts and being by my side in every important event of my life.

Last but not least, I would like to thank my family. Foremost, I would like to thank my mother, **Yianna,** for her devotion to me and my girls. Mom, thank you for not considering the long distance and expenses and being by our side when we needed it. I would like to thank my father, **Simos,** for all the support and all the days, weeks and months that he has been alone during my mother's visits to us. He has always supported my decisions and those of my brother, **Andreas,** even though most of the time he disagreed with them. I would like to thank my mother-in-law, **Emilia**, my godparents, **Toula** and **Marios,** and my grandmother, **Loulou,** for taking care of my children while I was writing this PhD thesis. You are the best!! I would like to thank my husband, **Yiannis,** for everything, for inspiring me, for believing in me and for bringing me to Sweden! But most of all I would like to thank my girls, **Ioanna** and **Emily,** for teaching me how to give and love unconditionally.

9 REFERENCES

1 Coffin A, Boulay-Coletta I, Sebbag-Sfez D, Zins M (2015) Radioanatomy of the retroperitoneal space. Diagn Interv Imaging 96:171-186

2 Gray H, Standring S (2005) Gray's anatomy : the anatomical basis of clinical practice. Elsevier Churchill Livingstone, Edinburgh

3 http://www.embryology.ch/anglais/sdigestive/pankreas01.html. Accessed 09.03.2015

4 Syed AB, Mahal RS, Schumm LP, Dachman AH (2012) Pancreas size and volume on computed tomography in normal adults. Pancreas 41:589-595

5 Saisho Y, Butler AE, Meier JJ et al (2007) Pancreas volumes in humans from birth to age one hundred taking into account sex, obesity, and presence of type-2 diabetes. Clin Anat 20:933-942

6 Horton KM, Fishman EK (2000) 3D CT angiography of the celiac and superior mesenteric arteries with multidetector CT data sets: preliminary observations. Abdom Imaging 25:523-525

7 Perez-Johnston R, Lenhart DK, Sahani DV (2010) CT angiography of the hepatic and pancreatic circulation. Radiol Clin North Am 48:311-330, viii

8 Crabo LG, Conley DM, Graney DO, Freeny PC (1993) Venous anatomy of the pancreatic head: normal CT appearance in cadavers and patients. AJR Am J Roentgenol 160:1039-1045

9 Balachandran A, Bhosale PR, Charnsangavej C, Tamm EP (2014) Imaging of pancreatic neoplasms. Surg Oncol Clin N Am 23:751-788

10 Cesmebasi A, Malefant J, Patel SD et al (2015) The surgical anatomy of the lymphatic system of the pancreas. Clin Anat 28:527-537

11 Malvezzi M, Arfe A, Bertuccio P, Levi F, La Vecchia C, Negri E (2011) European cancer mortality predictions for the year 2011. Ann Oncol 22:947-956

12 Vincent A, Herman J, Schulick R, Hruban RH, Goggins M (2011) Pancreatic cancer. Lancet 378:607-620

13 Hezel AF, Kimmelman AC, Stanger BZ, Bardeesy N, Depinho RA (2006) Genetics and biology of pancreatic ductal adenocarcinoma. Genes Dev 20:1218-1249

14 Gillen S, Schuster T, Meyer Zum Buschenfelde C, Friess H, Kleeff J (2010) Preoperative/neoadjuvant therapy in pancreatic cancer: a systematic review and meta-analysis of response and resection percentages. PLoS Med 7:e1000267

15 http://seer.cancer.gov/statfacts/html/pancreas.html. Accessed 10.03.2015

16 Garcea G, Dennison AR, Pattenden CJ, Neal CP, Sutton CD, Berry DP (2008) Survival following curative resection for pancreatic ductal adenocarcinoma. A systematic review of the literature. JOP 9:99-132

17 Tamm EP, Bhosale PR, Vikram R, de Almeida Marcal LP, Balachandran A (2013) Imaging of pancreatic ductal adenocarcinoma: State of the art. World J Radiol 5:98-105

18 Ansorge C, Strommer L, Andren-Sandberg A, Lundell L, Herrington MK, Segersvard R (2012) Structured intraoperative assessment of pancreatic gland characteristics in predicting complications after pancreaticoduodenectomy. Br J Surg 99:1076-1082

19 Fong ZV, Tan WP, Lavu H et al (2013) Preoperative imaging for resectable periampullary cancer: clinicopathologic implications of reported radiographic findings. J Gastrointest Surg 17:1098-1106
20 http://www.cancerresearchuk.org/cancer-help/type/pancreatic-cancer/about/pancreatic-cancer-symptoms. Accessed 10.03.2015
21 Siriwardena AK, Siriwardena AM (2014) Pancreatic cancer. BMJ 349:g6385
22 Martinez-Noguera A, D'Onofrio M (2007) Ultrasonography of the pancreas. 1. Conventional imaging. Abdom Imaging 32:136-149
23 Lee ES, Lee JM (2014) Imaging diagnosis of pancreatic cancer: a state-of-the-art review. World J Gastroenterol 20:7864-7877
24 Kulig P, Pach R, Kulig J (2014) Role of abdominal ultrasonography in clinical staging of pancreatic carcinoma: a tertiary center experience. Pol Arch Med Wewn 124:225-232
25 Putzer D, Jaschke W (2015) Radiological evaluation of focal pancreatic lesions. Dig Dis 33:91-98
26 Zamboni GA, Ambrosetti MC, D'Onofrio M, Pozzi Mucelli R (2012) Ultrasonography of the pancreas. Radiol Clin North Am 50:395-406
27 Faccioli N, Crippa S, Bassi C, D'Onofrio M (2009) Contrast-enhanced ultrasonography of the pancreas. Pancreatology 9:560-566
28 Nawaz H, Fan CY, Kloke J et al (2013) Performance characteristics of endoscopic ultrasound in the staging of pancreatic cancer: a meta-analysis. JOP 14:484-497
29 Fusaroli P, Kypraios D, Caletti G, Eloubeidi MA (2012) Pancreatico-biliary endoscopic ultrasound: a systematic review of the levels of evidence, performance and outcomes. World J Gastroenterol 18:4243-4256
30 Motosugi U, Ichikawa T, Morisaka H et al (2011) Detection of pancreatic carcinoma and liver metastases with gadoxetic acid-enhanced MR imaging: comparison with contrast-enhanced multi-detector row CT. Radiology 260:446-453
31 Koelblinger C, Ba-Ssalamah A, Goetzinger P et al (2011) Gadobenate dimeglumine-enhanced 3.0-T MR imaging versus multiphasic 64-detector row CT: prospective evaluation in patients suspected of having pancreatic cancer. Radiology 259:757-766
32 Holzapfel K, Reiser-Erkan C, Fingerle AA et al (2011) Comparison of diffusion-weighted MR imaging and multidetector-row CT in the detection of liver metastases in patients operated for pancreatic cancer. Abdom Imaging 36:179-184
33 Busireddy KK, AlObaidy M, Ramalho M et al (2014) Pancreatitis-imaging approach. World J Gastrointest Pathophysiol 5:252-270
34 Fukukura Y, Takumi K, Kamimura K et al (2012) Pancreatic adenocarcinoma: variability of diffusion-weighted MR imaging findings. Radiology 263:732-740
35 Sandrasegaran K, Nutakki K, Tahir B, Dhanabal A, Tann M, Cote GA (2013) Use of diffusion-weighted MRI to differentiate chronic pancreatitis from pancreatic cancer. AJR Am J Roentgenol 201:1002-1008
36 Wang XY, Yang F, Jin C, Fu DL (2014) Utility of PET/CT in diagnosis, staging, assessment of resectability and metabolic response of pancreatic cancer. World J Gastroenterol 20:15580-15589
37 Kauhanen SP, Komar G, Seppanen MP et al (2009) A prospective diagnostic accuracy study of 18F-fluorodeoxyglucose positron emission tomography/computed tomography, multidetector row computed tomography, and magnetic resonance imaging in primary diagnosis and staging of pancreatic cancer. Ann Surg 250:957-963

38 Chang JS, Choi SH, Lee Y et al (2014) Clinical usefulness of (1)(8)F-fluorodeoxyglucose-positron emission tomography in patients with locally advanced pancreatic cancer planned to undergo concurrent chemoradiation therapy. Int J Radiat Oncol Biol Phys 90:126-133
39 Izuishi K, Yamamoto Y, Sano T, Takebayashi R, Masaki T, Suzuki Y (2010) Impact of 18-fluorodeoxyglucose positron emission tomography on the management of pancreatic cancer. J Gastrointest Surg 14:1151-1158
40 Brennan DD, Zamboni GA, Raptopoulos VD, Kruskal JB (2007) Comprehensive preoperative assessment of pancreatic adenocarcinoma with 64-section volumetric CT. Radiographics 27:1653-1666
41 Raman SP, Fishman EK (2012) Advances in CT Imaging of GI Malignancies. Gastrointest Cancer Res 5:S4-9
42 Bockhorn M, Uzunoglu FG, Adham M et al (2014) Borderline resectable pancreatic cancer: a consensus statement by the International Study Group of Pancreatic Surgery (ISGPS). Surgery 155:977-988
43 Bronstein YL, Loyer EM, Kaur H et al (2004) Detection of small pancreatic tumors with multiphasic helical CT. AJR Am J Roentgenol 182:619-623
44 Lemke J, Schafer D, Sander S, Henne-Bruns D, Kornmann M (2014) Survival and prognostic factors in pancreatic and ampullary cancer. Anticancer Res 34:3011-3020
45 Arvold ND, Niemierko A, Mamon HJ, Fernandez-del Castillo C, Hong TS (2011) Pancreatic cancer tumor size on CT scan versus pathologic specimen: implications for radiation treatment planning. Int J Radiat Oncol Biol Phys 80:1383-1390
46 Kim JH, Park SH, Yu ES et al (2010) Visually isoattenuating pancreatic adenocarcinoma at dynamic-enhanced CT: frequency, clinical and pathologic characteristics, and diagnosis at imaging examinations. Radiology 257:87-96
47 Blouhos K, Boulas KA, Tselios DG, Katsaouni SP, Mauroeidi B, Hatzigeorgiadis A (2013) Surgically proved visually isoattenuating pancreatic adenocarcinoma undetected in both dynamic CT and MRI. Was blind pancreaticoduodenectomy justified? Int J Surg Case Rep 4:466-469
48 Prokesch RW, Chow LC, Beaulieu CF, Bammer R, Jeffrey RB, Jr. (2002) Isoattenuating pancreatic adenocarcinoma at multi-detector row CT: secondary signs. Radiology 224:764-768
49 Diehl SJ, Lehmann KJ, Sadick M, Lachmann R, Georgi M (1998) Pancreatic cancer: value of dual-phase helical CT in assessing resectability. Radiology 206:373-378
50 Zaheer A, Singh VK, Akshintala VS et al (2014) Differentiating autoimmune pancreatitis from pancreatic adenocarcinoma using dual-phase computed tomography. J Comput Assist Tomogr 38:146-152
51 Francis IR (2007) Pancreatic adenocarcinoma: diagnosis and staging using multidetector-row computed tomography (MDCT) and magnetic resonance imaging (MRI). Cancer Imaging 7 Spec No A:S160-165
52 Brook OR, Brook A, Vollmer CM, Kent TS, Sanchez N, Pedrosa I (2015) Structured Reporting of Multiphasic CT for Pancreatic Cancer: Potential Effect on Staging and Surgical Planning. Radiology 274:464-472
53 Al-Hawary MM, Francis IR, Chari ST et al (2014) Pancreatic ductal adenocarcinoma radiology reporting template: consensus statement of the Society of Abdominal Radiology and the American Pancreatic Association. Radiology 270:248-260
54 Parsons CM, Sutcliffe JL, Bold RJ (2008) Preoperative evaluation of pancreatic adenocarcinoma. J Hepatobiliary Pancreat Surg 15:429-435

55 Tamm EP, Balachandran A, Bhosale PR et al (2012) Imaging of pancreatic adenocarcinoma: update on staging/resectability. Radiol Clin North Am 50:407-428
56 Allen VB, Gurusamy KS, Takwoingi Y, Kalia A, Davidson BR (2013) Diagnostic accuracy of laparoscopy following computed tomography (CT) scanning for assessing the resectability with curative intent in pancreatic and periampullary cancer. Cochrane Database Syst Rev 11:CD009323
57 Shah D, Fisher WE, Hodges SE, Wu MF, Hilsenbeck SG, Charles Brunicardi F (2008) Preoperative prediction of complete resection in pancreatic cancer. J Surg Res 147:216-220
58 Lu DS, Reber HA, Krasny RM, Kadell BM, Sayre J (1997) Local staging of pancreatic cancer: criteria for unresectability of major vessels as revealed by pancreatic-phase, thin-section helical CT. AJR Am J Roentgenol 168:1439-1443
59 Varadhachary GR, Tamm EP, Abbruzzese JL et al (2006) Borderline resectable pancreatic cancer: definitions, management, and role of preoperative therapy. Ann Surg Oncol 13:1035-1046
60 <BB2.pdf>.
61 https://cancerstaging.org/references-tools/quickreferences/Documents/PancreasSmall.pdf.
62 Adsay NV, Bagci P, Tajiri T et al (2012) Pathologic staging of pancreatic, ampullary, biliary, and gallbladder cancers: pitfalls and practical limitations of the current AJCC/UICC TNM staging system and opportunities for improvement. Semin Diagn Pathol 29:127-141
63 Loyer EM, David CL, Dubrow RA, Evans DB, Charnsangavej C (1996) Vascular involvement in pancreatic adenocarcinoma: reassessment by thin-section CT. Abdom Imaging 21:202-206
64 Valls C, Andia E, Sanchez A et al (2002) Dual-phase helical CT of pancreatic adenocarcinoma: assessment of resectability before surgery. AJR Am J Roentgenol 178:821-826
65 Zhou Y, Zhang Z, Liu Y, Li B, Xu D (2012) Pancreatectomy combined with superior mesenteric vein-portal vein resection for pancreatic cancer: a meta-analysis. World J Surg 36:884-891
66 Lopez NE, Prendergast C, Lowy AM Borderline resectable pancreatic cancer: definitions and management. D - NLM: PMC4138454 OTO - NOTNLM
67 Tempero MA, Malafa MP, Behrman SW et al (2014) Pancreatic adenocarcinoma, version 2.2014: featured updates to the NCCN guidelines. J Natl Compr Canc Netw 12:1083-1093
68 Yeo CJ, Cameron JL, Sohn TA et al (1997) Six hundred fifty consecutive pancreaticoduodenectomies in the 1990s: pathology, complications, and outcomes. Ann Surg 226:248-257; discussion 257-260
69 Cullen JJ, Sarr MG, Ilstrup DM (1994) Pancreatic anastomotic leak after pancreaticoduodenectomy: incidence, significance, and management. Am J Surg 168:295-298
70 Bassi C, Dervenis C, Butturini G et al (2005) Postoperative pancreatic fistula: an international study group (ISGPF) definition. Surgery 138:8-13
71 Pratt WB, Callery MP, Vollmer CM, Jr. (2008) Risk prediction for development of pancreatic fistula using the ISGPF classification scheme. World J Surg 32:419-428
72 Roberts KJ, Hodson J, Mehrzad H et al (2014) A preoperative predictive score of pancreatic fistula following pancreatoduodenectomy. HPB (Oxford) 16:620-628

73 Frozanpor F, Albiin N, Linder S, Segersvard R, Lundell L, Arnelo U (2010) Impact of pancreatic gland volume on fistula formation after pancreatic tail resection. JOP 11:439-443
74 McNulty NJ, Francis IR, Platt JF, Cohan RH, Korobkin M, Gebremariam A (2001) Multi--detector row helical CT of the pancreas: effect of contrast-enhanced multiphasic imaging on enhancement of the pancreas, peripancreatic vasculature, and pancreatic adenocarcinoma. Radiology 220:97-102
75 Kidoh M, Nakaura T, Nakamura S et al (2013) Low-dose abdominal CT: comparison of low tube voltage with moderate-level iterative reconstruction and standard tube voltage, low tube current with high-level iterative reconstruction. Clin Radiol 68:1008-1015
76 Birnbaum BA, Hindman N, Lee J, Babb JS (2007) Multi-detector row CT attenuation measurements: assessment of intra- and interscanner variability with an anthropomorphic body CT phantom. Radiology 242:109-119
77 Gonzalez-Guindalini FD, Ferreira Botelho MP, Tore HG, Ahn RW, Gordon LI, Yaghmai V (2013) MDCT of chest, abdomen, and pelvis using attenuation-based automated tube voltage selection in combination with iterative reconstruction: an intrapatient study of radiation dose and image quality. AJR Am J Roentgenol 201:1075-1082
78 Schindera ST, Nelson RC, Mukundan S, Jr. et al (2008) Hypervascular liver tumors: low tube voltage, high tube current multi-detector row CT for enhanced detection--phantom study. Radiology 246:125-132
79 Nakayama Y, Awai K, Funama Y et al (2005) Abdominal CT with low tube voltage: preliminary observations about radiation dose, contrast enhancement, image quality, and noise. Radiology 237:945-951
80 Kim JE, Newman B (2010) Evaluation of a radiation dose reduction strategy for pediatric chest CT. AJR Am J Roentgenol 194:1188-1193
81 Leschka S, Stolzmann P, Schmid FT et al (2008) Low kilovoltage cardiac dual-source CT: attenuation, noise, and radiation dose. Eur Radiol 18:1809-1817
82 Dougeni E, Faulkner K, Panayiotakis G (2012) A review of patient dose and optimisation methods in adult and paediatric CT scanning. Eur J Radiol 81:e665-683
83 Schueller-Weidekamm C, Schaefer-Prokop CM, Weber M, Herold CJ, Prokop M (2006) CT angiography of pulmonary arteries to detect pulmonary embolism: improvement of vascular enhancement with low kilovoltage settings. Radiology 241:899-907
84 Marin D, Nelson RC, Barnhart H et al (2010) Detection of pancreatic tumors, image quality, and radiation dose during the pancreatic parenchymal phase: effect of a low-tube-voltage, high-tube-current CT technique--preliminary results. Radiology 256:450-459
85 Yanaga Y, Awai K, Nakayama Y et al (2007) Pancreas: patient body weight tailored contrast material injection protocol versus fixed dose protocol at dynamic CT. Radiology 245:475-482
86 Shinagawa M, Uchida M, Ishibashi M, Nishimura H, Hayabuchi N (2003) Assessment of pancreatic CT enhancement using a high concentration of contrast material. Radiat Med 21:74-79
87 Kim T, Murakami T, Takahashi S et al (1999) Pancreatic CT imaging: effects of different injection rates and doses of contrast material. Radiology 212:219-225
88 Heiken JP, Brink JA, McClennan BL, Sagel SS, Crowe TM, Gaines MV (1995) Dynamic incremental CT: effect of volume and concentration of contrast material and patient weight on hepatic enhancement. Radiology 195:353-357

89 Yamashita Y, Komohara Y, Takahashi M et al (2000) Abdominal helical CT: evaluation of optimal doses of intravenous contrast material--a prospective randomized study. Radiology 216:718-723
90 Bae KT, Heiken JP (2005) Scan and contrast administration principles of MDCT. Eur Radiol 15 Suppl 5:E46-59
91 Fleischmann D, Kamaya A (2009) Optimal vascular and parenchymal contrast enhancement: the current state of the art. Radiol Clin North Am 47:13-26
92 Fenchel S, Fleiter TR, Aschoff AJ, van Gessel R, Brambs HJ, Merkle EM (2004) Effect of iodine concentration of contrast media on contrast enhancement in multislice CT of the pancreas. Br J Radiol 77:821-830
93 Ma X, Setty B, Uppot RN, Sahani DV (2008) Multiple-detector computed tomographic angiography of pancreatic neoplasm for presurgical planning: comparison of low- and high-concentration nonionic contrast media. J Comput Assist Tomogr 32:511-517
94 Merkle EM, Boll DT, Fenchel S (2003) Helical computed tomography of the pancreas: potential impact of higher concentrated contrast agents and multidetector technology. J Comput Assist Tomogr 27 Suppl 1:S17-22
95 Schueller G, Schima W, Schueller-Weidekamm C et al (2006) Multidetector CT of pancreas: effects of contrast material flow rate and individualized scan delay on enhancement of pancreas and tumor contrast. Radiology 241:441-448
96 Ichikawa T, Erturk SM, Araki T (2006) Multiphasic contrast-enhanced multidetector-row CT of liver: contrast-enhancement theory and practical scan protocol with a combination of fixed injection duration and patients' body-weight-tailored dose of contrast material. Eur J Radiol 58:165-176
97 Tang A, Billiard JS, Chagnon DO et al (2014) Optimal Pancreatic Phase Delay with 64-Detector CT Scanner and Bolus-tracking Technique. Acad Radiol 21:977-985
98 Campbell F VC (2013) Pancreatic pathology - a practical approach. Springer London
99 Dindo D, Demartines N, Clavien PA (2004) Classification of surgical complications: a new proposal with evaluation in a cohort of 6336 patients and results of a survey. Ann Surg 240:205-213
100 Deak PD, Smal Y, Kalender WA (2010) Multisection CT protocols: sex- and age-specific conversion factors used to determine effective dose from dose-length product. Radiology 257:158-166
101 Dorfman DD, Berbaum KS, Metz CE (1992) Receiver operating characteristic rating analysis. Generalization to the population of readers and patients with the jackknife method. Invest Radiol 27:723-731
102 Obuchowski NA (2003) Receiver operating characteristic curves and their use in radiology. Radiology 229:3-8
103 Shrout PE, Fleiss JL (1979) Intraclass correlations: uses in assessing rater reliability. Psychol Bull 86:420-428
104 Altman DG, Bland JM (1983) Measurement in Medicine: The Analysis of Method Comparison Studies. The Statistician 32:307-317
105 Donahue TR, Isacoff WH, Hines OJ et al (2011) Downstaging chemotherapy and alteration in the classic computed tomography/magnetic resonance imaging signs of vascular involvement in patients with pancreaticobiliary malignant tumors: influence on patient selection for surgery. Arch Surg 146:836-843
106 Crippa S, Salvia R, Falconi M, Butturini G, Landoni L, Bassi C (2007) Anastomotic leakage in pancreatic surgery. HPB (Oxford) 9:8-15
107 Sakata N, Egawa S Fau - Rikiyama T, Rikiyama T Fau - Yoshimatsu G et al Computed tomography reflected endocrine function of the pancreas.

108 Frozanpor F, Loizou L, Ansorge C, Lundell L, Albiin N, Segersvard R (2014) Correlation between preoperative imaging and intraoperative risk assessment in the prediction of postoperative pancreatic fistula following pancreatoduodenectomy. World J Surg 38:2422-2429
109 Yeo TP (2015) Demographics, Epidemiology, and Inheritance of Pancreatic Ductal Adenocarcinoma. Semin Oncol 42:8-18
110 Metz CE (2006) Receiver operating characteristic analysis: a tool for the quantitative evaluation of observer performance and imaging systems. J Am Coll Radiol 3:413-422
111 Reiner CS, Karlo C, Petrowsky H, Marincek B, Weishaupt D, Frauenfelder T (2009) Preoperative liver volumetry: how does the slice thickness influence the multidetector computed tomography- and magnetic resonance-liver volume measurements? J Comput Assist Tomogr 33:390-397
112 McKay A, Mackenzie S, Sutherland FR et al (2006) Meta-analysis of pancreaticojejunostomy versus pancreaticogastrostomy reconstruction after pancreaticoduodenectomy. Br J Surg 93:929-936
113 Wang X, Misawa R, Zielinski MC et al (2013) Regional differences in islet distribution in the human pancreas--preferential beta-cell loss in the head region in patients with type 2 diabetes. PLoS One 8:e67454
114 Marin D, Boll DT, Mileto A, Nelson RC (2014) State of the art: dual-energy CT of the abdomen. Radiology 271:327-342
115 Klauss M, Stiller W, Pahn G et al (2013) Dual-energy perfusion-CT of pancreatic adenocarcinoma. Eur J Radiol 82:208-214
116 Primak AN, Ramirez Giraldo JC, Liu X, Yu L, McCollough CH (2009) Improved dual-energy material discrimination for dual-source CT by means of additional spectral filtration. Med Phys 36:1359-1369
117 D'Onofrio M, Gallotti A, Mantovani W et al (2013) Perfusion CT can predict tumoral grading of pancreatic adenocarcinoma. Eur J Radiol 82:227-233
118 Mileto A, Mazziotti S, Gaeta M et al (2012) Pancreatic dual-source dual-energy CT: is it time to discard unenhanced imaging? Clin Radiol 67:334-339
119 Macari M, Spieler B, Kim D et al (2010) Dual-source dual-energy MDCT of pancreatic adenocarcinoma: initial observations with data generated at 80 kVp and at simulated weighted-average 120 kVp. AJR Am J Roentgenol 194:W27-32